[10] Bailey A I ,Hayati I, Tadros T.F, Investigations into the mechanisms of electrohydrodynamic spraying of liquids. 1. Effect of electricfield and the environment on pendant drops and factors affecting the formation of stable jets and atomization. *Journal of Colloid and Interface Science* 1987, **117**, 205–221.

[11]Maneeprakorn W, Meejoo S, Winotai P, Phase and thermal stability of nanocrystalline hydroxyapatite prepared via microwave heating. *Thermochimica Acta* 2006, No. **447**, pp. 115–120

[12]Bernache-Assollante D, Champion E, Destainville A, Synthesis, characterization and thermal behaviour of apatite tricalcium phosphate // *Materials Chemistry and Physics* 2003, No. **80**, pp. 269 – 277

[13]Bernache-Assollant D, Champion E, Raynaud S, Calcium phosphate apatite with variable Ca/P atomic ratio I. Synthesis, characterisation and thermal stability of powders. *Biomaterials* 2002, No **23**, pp. 1065–1072

[14]Hong S H, Jun Y K, Kwon S H, Synthesis and dissolution behaviour of β- TCP and HA/β-TCP composite powders. *Journal of European Ceramic Society* 2003, No. **23**, pp. 1039–1045

[15]http://pubs.sciepub.com/wjee/3/4/1/figure/7

Sorumlu yazar:

Adı SOYADI: Erdi BULUŞ
Üniversite/Firma, Fakülte, Bölüm/Laboratuvar: Polimer Teknolojileri ve Kompozit Malzemeler Ar-Ge Merkezi, İstanbul Arel Üniversitesi, 34537 İstanbul, Türkiye.
E-mail: erdibulus@arel.edu.tr
Bildiri Sunumu (Türkçe/İngilizce): Türkçe Sözlü Sunum yapmak istiyorum.

Caustic soda treatment of electrospun cellulose acetate nanofibers for disperse dying

O Uslu, and H I Akyildiz, Y Aykut

Uludag University, Engineering Faculty, Textile Engineering Department, Nilufer, Bursa, Turkey, 16059

E-mail of the Presenting Author: aykut@uludag.edu.tr

ABSTRACT

Cellulose monoacetate nanofiber can be easily produced via electrospinning with desired morphology. However for the use of nanofibers for different applications it is desired to functionalize the surface of the fibers. Deacetylation of the acetate in order to change the surface chemistry is one way to enable functionalization and various approaches has been utilized for this purpose. In this study, cellulose monoacetate nanofibers were prepared via electrospinning method. As-spun nanofibers were treated with aqueous coustic soda solutions at different concentrations to vary the degree of acetylation in the nanofibers. As spun and coustic soda treated nanofibers were morphologically analyzed with electron microscopy (SEM). Degree of deacetylation was investigated with Fourier transform infrared spectroscopy (FTIR), which showed changes in the chemical structure of the polymer upon the coustic soda treatment. Thermal analysis of as-spun and coustic soda treated CA nanofibers were carried out with DSC method. Effect of caustic soda on cellulose acetate dying were carried out by dying as-spun nanofibers with a disperse dye and obtained reflectance values for interpretation.

INTRODUCTION

Nanofibers are promising materials which have very surface area to volume ratio. High specific surface are enhance the device performance to several order of magnitude when they are used in a specific device. Nanofibers have been produced from diversity of materials such as ceramics, polymers and metals and used for very broad applications including biomedical, energy and filtration (1). Silk fibroin (2), polyvynile alcohol (3), and poly (acrylonitrile-co-maleic acid) (4) nanofibers had been produced via electrospinning technique. Cellulose is a natural and obtained from variety of different sources such as tree, cotton and bacteria (5). Producing cellulose nanofibers is very challenge, because solubility of natural cotton is very difficult. Cellulose acetate can be dissolve in an appropriate solvent. When CA is dissolved with a proper molecular weight and concentration, the solution can be electrospun nanofibrous structure. Then, as-spun CA nanofibers can be converted to cellulose nanofibers by deactylatin. There are various deactylation techniques in the literature such as NaOH(6), by fluorination (7) , benzene/acetic acid/water system (8), metal salt(9), etc. Preperation of cellulose based nanofibers have been reported by different studies in the literature. (5,10,11). Prasetyo et al. treated cellulose acetate to properly functionalize with laccase and the removal of toxic combustion products (12). Cellulose acetat nanofibers dying with disperse dyes were conducted by Khatri et al. (13). In this study, we fabricated cellulose acetate nanofibers, and treated as-spun nanofibers with coustic soda. As-spun and coustic soda treated CA nanofibers were characterized with SEM, FTIR and DSC methods. Effect of caustic soda on cellulose acetate dying with disperse dyes were carried out.

EXPERIMENTAL

Materials: Cellulose monoacetate (CMA, Aldrich, Mn~30.000), coustic soda, acetone and distilled water were used as chemical.

Methods: Multi nozzle electrospinning process was conducted to produce CA nanofibers. Schematic illustration of multi nozzle electrospinning is demonstrated in Figure 1. 15 wt% of CA/aseton solution is perpared by magnetically stirring for 24 hours in an ambient condition. Then the stock solution was

loaded in a plastic syringes fitted with a stainless steel needle. Cylindrical grounded collector was stayed in front of the needle where polymer soltion is fet. After applicaiton of high voltage polymer droplets were ejected to the collector, acetone was evaporated and the dried CA nanofibers were collected on the cylindrical collector.

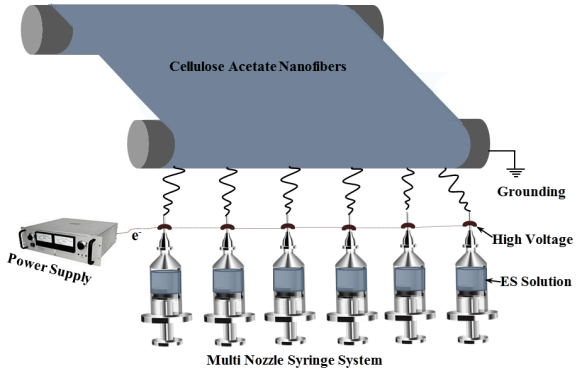

Figure 1. Schematic illustration of multi nozzle electrospinning system.

Different concenration of coustic soda/water solutions were prepared in seperated glass vials in an ambient condition. As-spun nanofibers were soaked in the prepared soltions and stayed about 15 seconds then washed with deionized water several times and dried for characterizaitons. Morphologies of nanofibers were analysed with a scanning electron microscopy (SEM). Chemical analysis were conducted with an attenuated total reflectance fourier transform infrared spectroscopy (ATR-FTIR). Thermal characterizations were carried out by differential scanning calorimeter (DSC). For dying samples, as-spun nanofibers were coated on cotton weaved fabrics for an appropriate dying. Because only cellulose acetate were dyed with the disperse dye, weaved cellulose fabric substrate was selected.

Dying start at room temperature and temperature gradually increase up to 130 ^{o}C in 45 minutes. When the temperature reached to 130 ^{o}C, samples were taken from the dying chamber and gentely washed with cold water. Then, the samples were dried and reflectance measurement were conducted.

RESULTS and DISCUSSION

Morphological analtsis of as-spun and coustic soda treated cellulose acetate nanofibers were condected by SEM imaging technique and demonstrated in Figure 2. As seen from Figure 2A and 2B, as-spun CA nnaofibers show uniforms 3D nanofibrous networking structure in a mat. When as-spun Ca nanofibers were treated with coustic soda, fiber uniform is lost and fiber morphology transforms to fuzzed structure (Figure 2C and 2D). Avarage fibers diameter increases after cosutic soda treatment, since the fibers swell and damage a little bit.

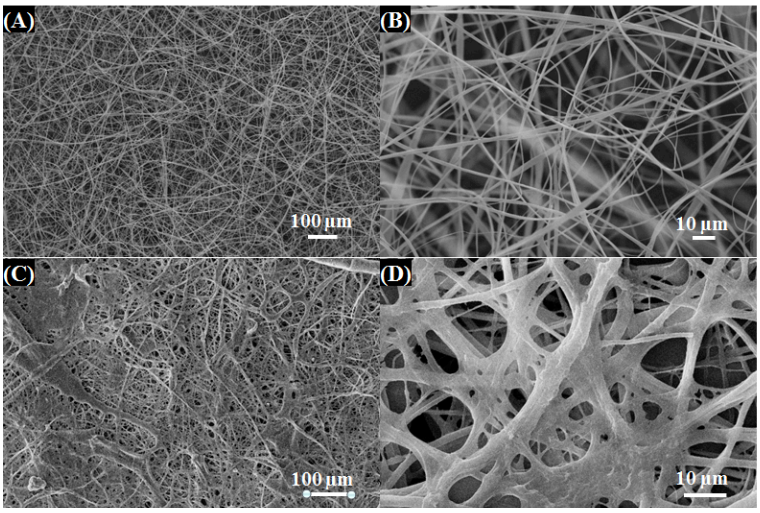

Figure 2. SEM images of (A, B) CA nanofibers, (C, D) coustic soda treated CA nanofibers.

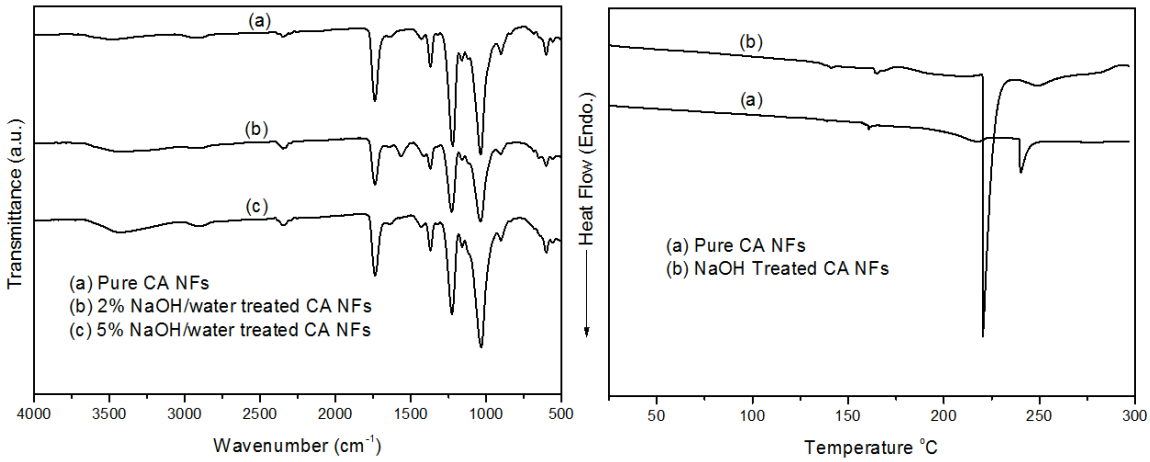

Figure 3. ATR-FTIR and DSC spectra of pure and coustic soda treated CA nanofibers: (A) Left graph: ATR-FTIR Spectra, and (B) Rigth graph DSC spectra.

Figure 3(left) shows FTIR spectra of the produced pure abd coustic soda treated CA nanofibers, respectively. In pure CA nanofibers, strong peaks at 1739 cm-1 (C=O from acetyl groups) which is an carbonyl absorbtion band correspond to acetyl group. Also, peaks at 1037 and 1222 cm^{-1} (C-O-C), and 1369 cm^{-1} (C-CH_3) come from CMA nanofibers (14). There is no distinctive difference between the neat CA and coustic soda treated CA nanofiber samples. The intensity band between 3000-3750 (OH group) increase with cpostic soda treatment. DSC thermograms of the as-spun and coustic soda treated CA nanofibers were recorded at temperatures ranging from 25 to 300 °C and demonstrated im Figure 2 (right). The freshly electrospun CMA nanofibers exhibit a relatively strong exothermic peak centered at ca. 230 °C, which is associated with Tm of CA NFs (15). Tg of CA observed at around160 ^{o}C (16). With coustic soda treatment CA nanofiber Tm go higher and Tg go to lower temperature.

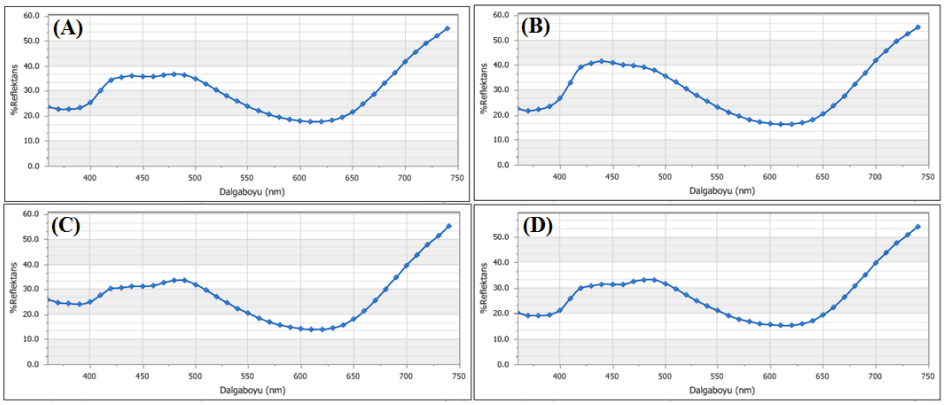

Figure 4. Percent reflectances of cellulose acetate nanofiber coated cotton fabric caustic soda treated and dyed with a blue disperse dye: a) pure, b) low caustic, c)middle concentration of caustic, and d) high concentration caustic treatment before dying.

When the reflectance values were compared, reflectance values of all the samples are close to each other except low concentration of caustic treated sample. A little enhancement was observed for low concentration of caustic treated sample and a very small reduction of reflectance value was observed at high concentration of caustic treated sample. It can be speculated that low concentration of caustic treatment to cellulose acetate nanofibers before disperse dying is preferable. On the other hand, it should be avoided high concentration caustic treatment of cellulose acetate nanofibers because nanofibers are destroyed and their uniformity can be totally lost.

CONCLUSIONS

Cellulose acetate nanofibers successfully produced in an ambient condition via electrospinning technique by using acetone as solvent. As-spun nanofibers were treated with coustic soda. SEM images reveals that coustic soda treatment causes to conversion of uniform nanofibers morphology to fuzed structure. After investigating FTIR results, no distinct deactylation were observed as-expected. DSC result reveals that Tm decrease and Tg increases with caustic soda treatment. Reflectance values of pure, low, mid and high caustic soda concentration treated cellulose acetate nanofibers were close to each other.

ACKNOWLEDGMENTS

The study presented here is a part of Oguzhan Uslu's Master thesis work at Graduate School of Natural and Applied Sciences, Uludag University.

REFERENCES

1. Bhardwaj N, Kundu SC. Electrospinning: A fascinating fiber fabrication technique. Vol. 28, Biotechnology Advances. 2010. p. 325–47.
2. Lee KH, Ki CS, Baek DH, Kang GD, Ihm D-W, Park YH. Application of electrospun silk fibroin nanofibers as an immobilization support of enzyme. Fibers Polym. 2005;6(3):181–5.
3. Wang Y, Hsieh YL. Immobilization of lipase enzyme in polyvinyl alcohol (PVA) nanofibrous membranes. J Memb Sci. 2008;309(1–2):73–81.
4. Ye P, Xu ZK, Wu J, Innocent C, Seta P. Nanofibrous poly(acrylonitrile-co-maleic acid) membranes functionalized with gelatin and chitosan for lipase immobilization. Biomaterials. 2006;27(22):4169–76.
5. Liu Y, Chen JY. Enzyme immobilization on cellulose matrixes. J Bioact Compat Polym

[Internet]. SAGE Publications; 2016 Nov 1 [cited 2016 Dec 11];31(6):553–67. Available from: http://jbc.sagepub.com/cgi/doi/10.1177/0883911516637377

6. Liu H, Hsieh Y Lo. Ultrafine fibrous cellulose membranes from electrospinning of cellulose acetate. J Polym Sci Part B Polym Phys. 2002;40(18):2119–29.

7. Kim M Il, Lee YS. Deacetylation of cellulose acetate nanofibers by fluorination for carbon nanofibers. Mater Lett. 2016;181:236–9.

8. Olaru N, Olaru L. Cellulose acetate deacetylation in benzene/acetic acid/water systems. J Appl Polym Sci [Internet]. Wiley Subscription Services, Inc., A Wiley Company; 2004 Dec 5 [cited 2017 Mar 23];94(5):1965–8. Available from: http://doi.wiley.com/10.1002/app.21035

9. Murphy AP. Accelerated Deacetylation of Cellulose Acetate by Metal Salts with Aqueous Chlorine. Res J Water Pollut Control Fed [Internet]. 1991;63(2):177–80. Available from: http://www.jstor.org/stable/25043973

10. Sulaiman S, Mokhtar MN, Naim MN, Baharuddin AS, Sulaiman A. A Review: Potential Usage of Cellulose Nanofibers (CNF) for Enzyme Immobilization via Covalent Interactions. Appl Biochem Biotechnol. 2014;175(4):1817–42.

11. Sathishkumar P, Kamala-Kannan S, Cho M, Kim JS, Hadibarata T, Salim MR, et al. Laccase immobilization on cellulose nanofiber: The catalytic efficiency and recyclic application for simulated dye effluent treatment. J Mol Catal B Enzym. 2014;100:111–20.

12. Prasetyo EN, Semlitsch S, Nyanhongo GS, Lemmouchi Y, Guebitz GM. Laccase functionalized cellulose acetate for the removal of toxic combustion products. React Funct Polym [Internet]. 2015 Dec [cited 2017 Mar 22];97:12–8. Available from: http://linkinghub.elsevier.com/retrieve/pii/S1381514815300523

13. Khatri Z, Khatri A, Saleem U, Mayakrishnan G, Kim BS, Wei K, Kim IS. Pad dyeing of cellulose acetate nanofibres with disperse dyes, Color. Technol., 2012; 129, 159–163.

14. Rodríguez K, Renneckar S, Gatenholm P. Biomimetic calcium phosphate crystal mineralization on electrospun cellulose-based scaffolds. ACS Appl Mater Interfaces. 2011;3(3):681–9.

15. Ma Z, Kotaki M, Ramakrishna S. Electrospun cellulose nanofiber as affinity membrane. J Memb Sci. 2005;265(1–2):115–23.

16. Vallejos ME, Peresin MS, Rojas OJ. All-Cellulose Composite Fibers Obtained by Electrospinning Dispersions of Cellulose Acetate and Cellulose Nanocrystals. J Polym Environ [Internet]. Springer US; 2012 Dec 1 [cited 2017 Jan 30];20(4):1075–83. Available from: http://link.springer.com/10.1007/s10924-012-0499-1

Corresponding author:

Yakup AYKUT, Uludag University, Faculty of Engineering, Department of Textile Engineering, 16059, Nilufer, Bursa, Turkey.
Tel: +90 224 294 07 67, E-mail: aykut@uludag.edu.tr

Presentation options to indicate

1. Indicate your preference for the presentation: ***Oral***

2. Indicate the preference for the ***conference topic****: Ar-Ge/Ur/Ge*

Grafen Kaplı Poliamid Mono Filament İpliklerin Üretimi ve Elektriksel, Optik ve Morfolojik Özelliklerinin Araştırılması

Mahmut TAŞ[1,2], Yasin ALTIN[1], Ayşe BEDELOĞLU[1]

[1]Bursa Teknik Üniversitesi, Lif ve Polimer Mühendisliği Bölümü, BURSA

[2]Çukurova Üniversitesi, Tekstil Mühendisliği Bölümü, ADANA

E-Mail: mahmuttas@cu.edu.tr, yasin.altin@hotmail.com, ayse.bedeloglu@btu.edu.tr

ÖZET

Bu çalışma kapsamında grafen oksit nanomateryali modifiye edilmiş hummers metodu ile üretilmiş ve FT-IR analizi ile karakterizasyonu sağlanmıştır. Üretilen grafen oksit, monofilament iplik yüzeyine daldırma yöntemi ile 4 farklı daldırma sayısında kaplanmış, böylece yüzeye tutunan grafen oksit miktarının değişiminin monofilament ipliğin özelliklerine etkisi araştırılmıştır. Grafen oksit, kaplama işleminin ardından çok adımlı indirgeme yöntemi ile lif yüzeyinde grafene dönüştürülmüştür. Bu indirgeme çalışması sırasıyla kimyasal ve termal indirgeme yöntemleri aracılığıyla gerçekleştirilmiş ve grafen oksit üzerinde bulunan fonksiyonel grupların uzaklaşması sağlanarak iletkenlik özelliklerinin gelişmesi sağlanmıştır. Üretilen ipliklerin daha sonra optik, elektriksel ve görüntü analizleri gerçekleştirilecektir. Çalışma kapsamında üretilen ipliklerin giyilebilir tekstiller ve süper kapasitörler için elektrot olarak kullanılabileceği öngörülmektedir.

Investigation of electrical, optical and morphological properties of graphene coated polyamide monofilament yarns

Mahmut TAŞ[1,2], Yasin ALTIN[1], Ayşe BEDELOĞLU[1]

[1]Bursa Technical University, Department of Fiber and Polymer Engineering, Yildirim/Bursa, Turkey

[2]Çukurova University, Textile Engineering Department, Balcalı, 01330, Yüreğir / ADANA

E-mail address: (mahmuttas@cu.edu.tr , yasin.altin@hotmail.com, ayse.bedeloglu@btu.edu.tr)

ABSTRACT

In this study, graphene oxide nanomaterial was produced by modified hummers method and characterized by FT-IR analysis. The graphene oxide produced was coated with 4 different dipping numbers by immersion method on the monofilament yarn surface so that the effect of the amount of graphene oxide adhering to the surface on the properties of the monofilament yarn was investigated. Graphene oxide is transformed into graphene on the fiber surface by the multi-step reduction method after coating. This reduction work was carried out by means of chemical and thermal reduction methods, respectively, and the conductivity properties were improved by the removal of the functional groups on the graphene oxide. The produced yarns will then be subjected to optical, electrical and image analysis. It is envisaged that the yarns produced in the scope of the study can be used as electrodes for wearable textiles and supercapacitors.

1. Giriş

Grafen iki boyutlu olduğu kabul edilen ve karbon atomlarının altıgen balpeteği örgüsünde kusursuz olarak dizilmesi ile oluşan bir nanomateryaldir[1]. Sahip olduğu geniş yüzey alanı, elektriksel iletkenlik, mukavemet ve yüksek ısıl iletkenlik gibi üstün özellikler ile grafen bir çok uygulama alanı bulmuştur[2]. Üretim yöntemlerindeki çeşitlilik ve kolay üretilebilirlik de grafen nanomateryalinin yaygınlaşmasında önemli bir etken olarak düşünülebilir. Tekstil sektörü de grafen ve grafen oksit

nanomateryalinin kullanım alanlarından birini oluşturmakta ve literatür incelendiğinde liften kumaşa ve bitim işlemlerine kadar bir çok çalışma adımında farklı fonksiyonel özellikler sağlamak için kullanıldığı görülmektedir[3-5]. Bu kullanımların başlıcaları tekstil yüzeyine iletkenlik sağlamak, mukavemet özelliklerini iyileştirmek ve oksitlenmiş grafen formuyla tekstil yüzeylerine antibakteriyellik sağlamak olarak özetlenebilir[6].

Bu çalışmada grafen oksit nanomateryali sulu çözelti halinde daldırma yöntemi esasına göre poliamid monofilament ipliğe uygulanmıştır. Uygulama sonucunda monofilament ipliğe ait optik, elektriksel ve morfolojik değişimler araştırılmıştır. Çalışma sonucunda monofilament ipliklerin iletkenlik özelliği kazandığı tespit edilmiş ve optik özelliklerindeki değişimler analiz edilmiştir.

2. Materyal ve Metod

Grafen oksit sentezi

Grafen oksit, grafit hammaddesinden modifiye edilmiş hummers metodu ile üretilmiştir. Bu metoda göre ilk 9:1 oranın sülfürik asit ve fosforik asit karışımı hazırlanmıştır. Ardından bu karışıma 3 gr grafit tozu eklenmiş ve bir süre homojenleşmesi beklenmiştir. Daha sonra 1:6 grafit / potasyum permanganat oranı oluşturacak şekilde (18 gr) potasyum permanganat buz banyosu içerisine alınan karışıma yavaş yavaş eklenmiştir. Potasyum permanganat ilavesi tamamlandığında çözelti ısıtmalı karıştırıcı üzerine alınmış ve 50 derece sıcaklığa ısıtılmıştır. Bu karışım en az 12 saat sabit karıştırma altında beklenmiştir. Son olarak eklenen 3 ml Hidrojen peroksit ile reaksiyon sonlandırılmıştır. Üretilen grafen oksit santrifüj ile pH 6.5-7 aralığına ulaşıncaya kadar saf su ile yıkama yapılmış ardından karakterizasyon işlemlerine geçilmiştir.

Poliamid monofilament ipliğe grafen oksit nanomateryalinin uygulanması

Üretilen grafen oksit nanomateryali poliamid monofilament ipliğe daldırma metodu ile uygulanmıştır. Daldırma sayısı değişken olarak kabul edilmiş ve 1, 3, 5 ve 7 defa daldırma yapılarak farklı kalınlıkta kaplamalar elde edilmiştir. Her bir deney 6 defa tekrarlanmış ve bu 6 numunenin yarısı grafen oksit kaplı poliamid monofilament olarak analiz edilirken, kalan yarısına çok adımlı indirgeme işlemi uygulanmıştır. Hazırlanan deney seti tablo 1'de verilmiştir.

Tablo 1: Hazırlanan deney seti

Daldırma sayısı	Grafen oksit kaplı numune sayısı	İndirgeme işlemi uygulanmış nunume sayısı
0	3	3
1	3	3
3	3	3
5	3	3
7	3	3

Grafen oksitin Poliamid yüzey üzerinde indirgenmesi

Üretilen numunelerin indirgenmesi işlemi askorbik asit ile yapılmıştır. Askorbik asitin 1 molar konsantrasyona kadar poliamide zarar vermediği görülmüştür. İndirgeme için 400 milimolar konsantrasyonda çözelti hazırlanmış ve üretilen numuneler 90 derece sıcaklıktaki bu çözeltiye 5'er dakika daldırılmıştır. Daldırma sonrası numune renklerinin kahverengiden siyaha döndüğü görülmüştür. Ardından 120 dereceye ayarlanmış fırında 15 dakika ısıtma işlemi ile indirgeme tamamlanmıştır.

3. Sonuçlar

Üretilen grafen oksite ait FT-IR spektrumu şekil 1'de görülmektedir. 3200 cm^{-1} dalga sayısında –OH vibrasyon piki, 1782 cm^{-1}'de C=O piki, 1619 cm^{-1}'de C=C vibrasyon piki, 1362 cm^{-1}'de C-O piki görülmektedir. Sonuçlar irdelendiğinde grafit hammaddesinin başarılı bir şekilde oksitlendiği görülmektedir.

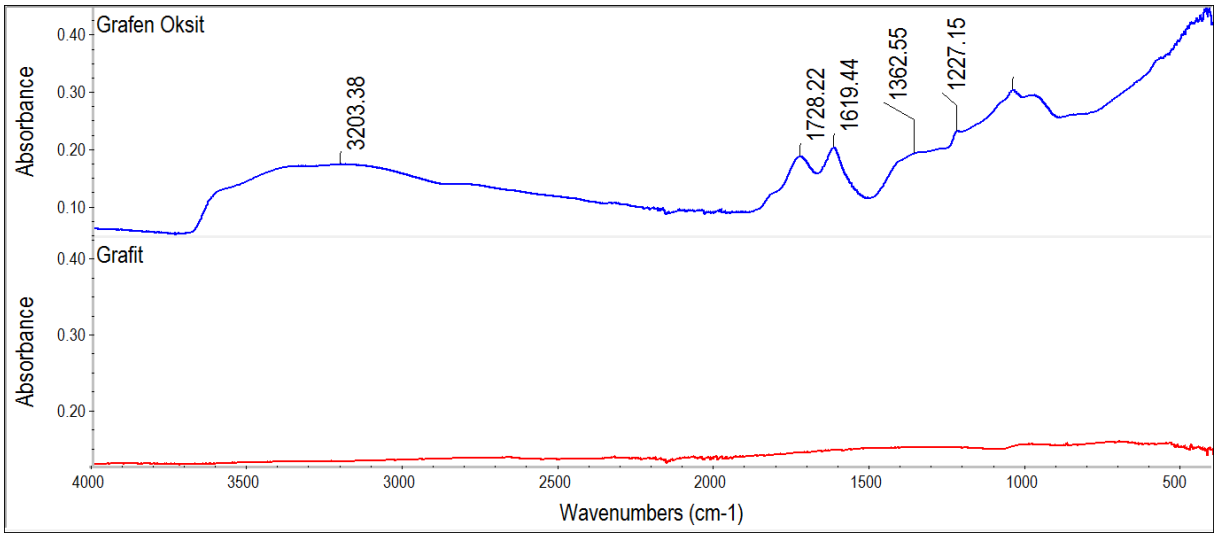

Şekil 1: Grafit ve grafen oksit FT-IR spektrumu.

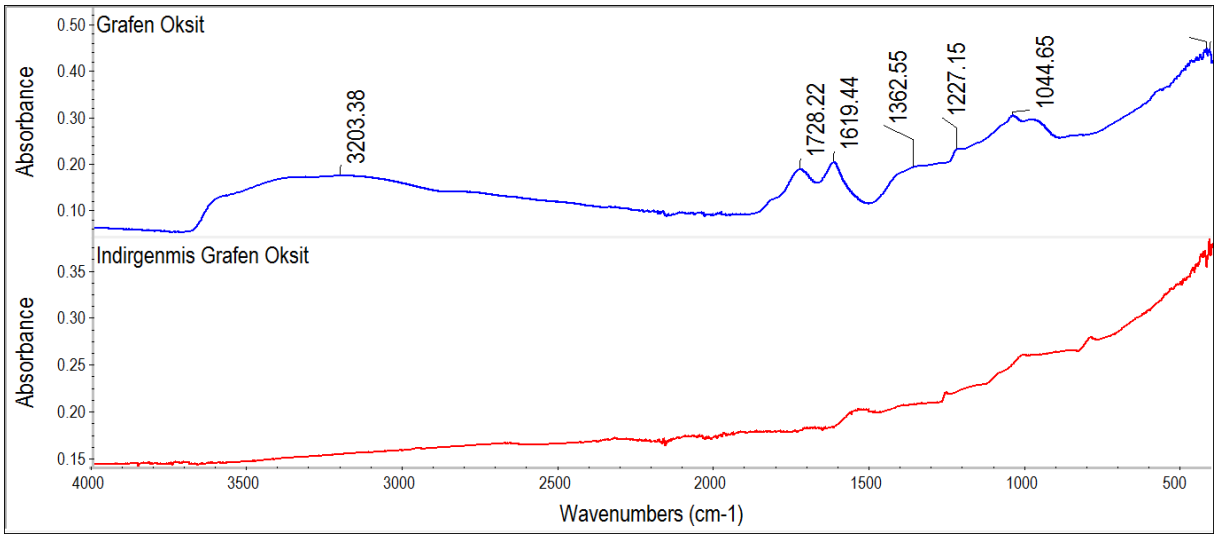

Şekil 2: Grafen oksit ve indirgenmiş grafen oksit FT-IR spektrumu.

Şekil 2'de grafen oksitin askorbik asit ile indirgenmesinden sonraki FT-IR spektrumu görülmektedir. Şekilde görüldüğü gibi fonksiyon grupların indirgeme işlemi sonunda uzaklaştırılarak başarılı bir şekilde indirgendiği görüşmektedir.

Üretilen Grafen oksit ve indirgenmiş grafen oksit kaplı numunelerin görüntüsü şekilde verilmiştir. Yüzeyde tutunan grafen oksit miktarı arttıkça ipliklerin görünümünün açık kahve rengiden koyu kahverengiye dönüştüğü, indirgeme işlemi ardından ise griden siyaha dönüştüğü görülmektedir.

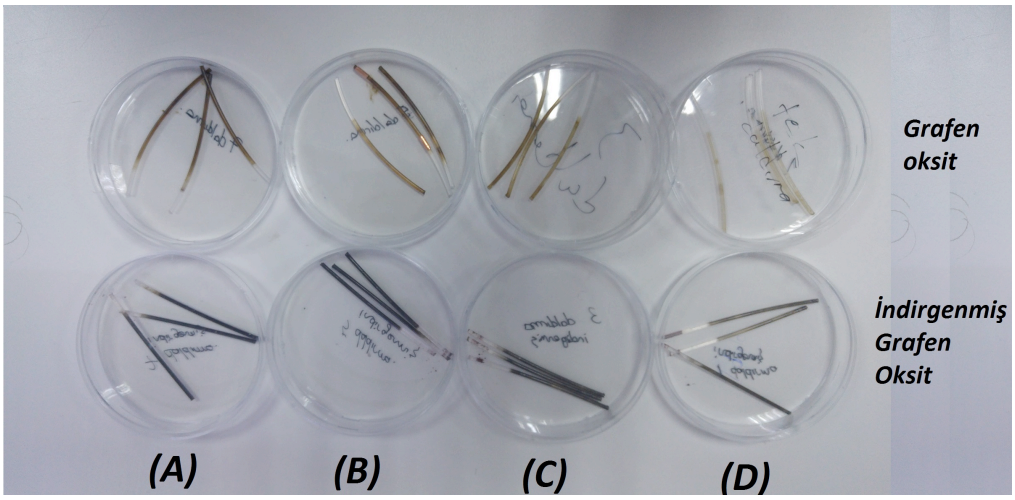

Şekil 3: (A) 7, (B) 5, (C) 3 ve (D) 1 defa daldırma işlemi uygulanmış numuneler

Referanslar

1. Allen, M.J., V.C. Tung, and R.B. Kaner, *Honeycomb Carbon: A Review of Graphene.* Chemical Reviews, 2010. **110**(1): p. 132-145.
2. Shams, S.S., R.Y. Zhang, and J. Zhu, *Graphene synthesis: a Review.* Materials Science-Poland, 2015. **33**(3): p. 566-578.
3. Neves, A.I.S., et al., *Transparent conductive graphene textile fibers.* Scientific Reports, 2015. **5**.
4. Sahito, I.A., et al., *Graphene coated cotton fabric as textile structured counter electrode for DSSC.* Electrochimica Acta, 2015. **173**: p. 164-171.
5. Jalili, R., et al., *Scalable One-Step Wet-Spinning of Graphene Fibers and Yarns from Liquid Crystalline Dispersions of Graphene Oxide: Towards Multifunctional Textiles.* Advanced Functional Materials, 2013. **23**(43): p. 5345-5354.
6. Zhao, J.M., et al., *Graphene Oxide-Based Antibacterial Cotton Fabrics.* Advanced Healthcare Materials, 2013. **2**(9): p. 1259-1266.

Tourmaline/Polypropylene Filament Production for Energy Generating Smart Textiles

D VATANSEVER BAYRAMOL [1]

[1]Namık Kemal University, Corlu Faculty of Engineering, Department of Textile Engineering,

Silahtaraga Mah. Universite 1. Sok. No:13 Corlu-Tekirdag, Turkey

dvbayramol@nku.edu.tr

ABSTRACT

Textile is a slightly new application area for piezoelectric materials which are capable of converting mechanical energy to electrical energy and vice versa. The reason is that some of them are not amenable for use in large surface areas or in complex shapes. However, polymeric materials are good candidates for production of large surface areas and any shapes. Their high mechanical strength and high impact resistance makes them desirable for a number of applications. In this work, the production of tourmaline (TM) added polypropylene (PP) has been given in details. The direct piezoelectric properties of PP/TM filaments have been investigated. TM nanoparticles were dispersed into the PP polymer via a twin-screw melt compounder for production of PP/TM masterbatches which were then extruded from melt and poled simultaneously to form piezoelectric filaments. The poling of the polymers was carried out in drawing area, at an elevated temperature. The filaments were subjected to a high voltage while they were being stretched in drawing area. The thermal characteristic of the produced filaments were studied via a Differential scanning calorimetry (DSC). The crystallinity of the materials were calculated. Produced piezoelectric filaments were then sandwiched in between two aluminium sheets and subjected to an impact. The voltage generation characteristics of poled pristine PP and PP/TM filaments were comparatively investigated. The results confirmed that both polymeric filaments exhibited piezoelectric property after poled at certain conditions and generated voltage when subjected to an external stimulus. However, peak voltage generation of PP/TM filaments was recorded to be slightly higher than that of pristine PP filaments. It can be concluded that since produced materials are in filament form, flexible light weight and easy to process, they can be easily used to produce textile structures for energy harvesting smart textile applications.

INTRODUCTION

Due to the increase in global population and development of electronic devices with several functions, energy demand increases dramatically. Researchers from various disciplines have been working on the production of efficient and effective renewable energy to eliminate or at least decrease the amount of coal and oil used. Renewable energy can be produced by certain smart materials which can convert environmental stimuli to electrical energy. These external stimuli can be pressure, temperature, vibration, wind, light and so on.

Piezoelectric materials are one of those smart materials which can convert different types of applied stimulus to electrical energy. Materials with piezoelectricity are able to convert mechanical energy to electrical energy and, conversely, electrical energy to mechanical energy. This phenomenon was first discovered by Curie brothers in 1880 [1]. What they first discovered was “direct piezoelectric effect” which states formation of an electrical charge as a result of applied mechanical energy.

The molecular structure of a piezoelectric material is oriented such that the material exhibits a local charge separation, known as electric dipoles which are randomly oriented in man-made piezoelectric materials. The orientation of these electrical dipoles are more uniform in naturally occurring piezoelectric material while man-made piezoelectric materials such as ceramic-based and polymer-based piezoelectric materials need to be undergone certain mechanical, electrical and thermal conditions. Due to the application of a strong electrical field, electrical dipoles in a ceramic and/or polymer material reorient themselves. This process is called as poling. Once the polarisation is

extinguished, the electric dipoles maintain their position as shown in Figure 1 and the material exhibits piezoelectric effect. It should be noted that the alignment of the dipole moments may not be perfectly straight since each domain may have several allowed directions.

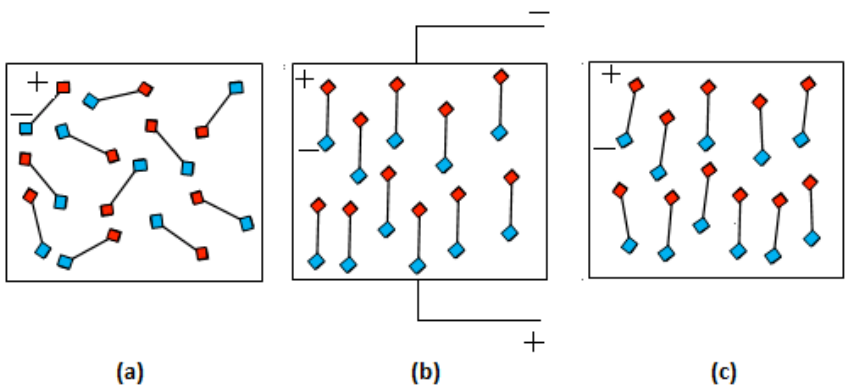

Figure 1. Orientation of dipoles, (a) random orientation of dipoles, (b) orientation of dipoles during polarisation, (c) remnant polarisation after the electric field is extinguished.

Four essential criteria for piezoelectric behaviour were reported by Broadhurst et al. [2] that are (1) presence of molecular dipoles, (2) the ability to align the dipole moments, (3) the locking-in of dipole alignment and its subsequent stability and (4) the ability of the material to strain with applied stress. However, it should be noted that these dipoles can keep their alignment unless they are heated to Curie temperature (Tc). This is the temperature at which polarisation is lost and the dipoles becomes randomly oriented again.

Materials which exhibit piezoelectric effect inherently are some natural materials and crystals. Efforts on practical application of piezoelectric materials were mainly made in the beginning of the 20th century, more particularly during the World War I. One of the early applications was a transducer made of piezoelectric quartz for underwater echo ranging and depth sounding to detect submarines [3] that became a commercial product in Great Britain and the United States after the War. Other application examples of piezoelectric crystals are including but not limited to loudspeakers, microphones, telephone receivers, photograph pick-ups etc. [4].

In the mid of 18th century, it was discovered that some ceramics could be made piezoelectric when subjected to a large electric field at an elevated temperature while the first discovery of the man-made piezoelectric polymers was announced by Kawai in 1969 [5] although it had been considered earlier by Brain [6] and Fukada [7]. It was expected that polymeric piezoelectric materials would overcome the drawbacks of ceramic-based piezoelectric materials due to having high mechanical strength and high impact resistance.

Polypropylene (PP) is a thermoplastic polymer with a repeating unit of [–CH_2–$CH(CH_3)$–]. It is also one of the most widely used polymer due to its high durability, high mechanical strength, temperature resistance, good chemical resistance. PP can be found in three types; atactic, isotactic and syndiotactic [8-10]. Isotactic PP is a polymorphic semi-crystalline material with an intermediate level of crystallinity which is highly dependent upon the temperature of the melt and processing conditions.

Three known crystalline forms of isotactic PP are alpha (α-), beta (β-) and gamma (γ-) phases [11-13]. The most prevalent crystalline form in commercially available isotactic PP is non-polar α-phase. With the use of special processing conditions such as a drawing and poling, polar phases, β- and γ-, can be achieved. Piezoelectric effect of polymeric materials is much related to the degree of polarisation achieved. A strong electric field should be applied to the polymer at an elevated temperature in order to induce polarisation [14]. However, other factors, like addition of different particles, can have an effect to influence the piezoelectric property of a polymeric material.

In this study, tourmaline (TM) nanoparticles were added into PP polymer via a twin-screw melt compounder for production of PP/TM masterbatches. Prepared masterbatches were then extruded from

melt and poled simultaneously to form piezoelectric filaments. The PP/TM polymer composite monofilament was polled at an elevated temperature in drawing area. Applied DC high voltage was 15kV for the polarisation process. Produced piezoelectric monofilaments were characterised by using FTIR and DSC. The crystallinity of the materials were calculated from the melting enthalpies collected from DSC thermograms. Small samples were produced by aligning piezoelectric monofilaments between two aluminium sheets and the samples were subjected to an impact. The voltage generation characteristics of poled pristine PP and PP/TM filaments were comparatively investigated.

EXPERIMENTAL

Materials

Polypropylene is a thermoplastic polymer consisting carbon and hydrogen atoms with a chemical formula of $(C_3H_6)_n$. PP pellets with 171°C melting point, 25g/10min (230°C/2.16kg) melt flow rate and 34cm^3/10min (230°C/2.16kg) melt volume flow rate used for piezoelectric fibre production were provided by Lyondellbasell Polymers.

Tourmaline is a crystal material which is known as inherently piezoelectric. However, only limited works and information are available for its piezoelectric effect. Tourmaline powder used in this study was obtained from Shanghai HuZheng NanoTechnology Company (China).

Methods

PP/TM masterbatches containing 1% TM into polymer matrix was prepared by using a twin-screw melt compounder [15]. The temperature of the heating zone, consists of six parts, is increased gradually from 170°C to 210°C. The torque of the double-screw needs to be kept below 80% to avoid any blockage. Therefore, the parameters applied for compounding were 10% feeding rate and 250 rpm twin-screw rotation speed which helps to keep the torque below 80%. PP granules and TM particles were fed together to the compounder. Granular polymer melts during the travel in six temperature controlled zones including feeding barrel and the die. TM particles get dispersed into the molten polymer between feeding unit and the die. Extruded single filament passes through a cold water bath for cooling and then dried via a blower just before the cutting unit where the single filament is cut into small pieces as granules. Produced masterbatches were then dried at 80ºC in the oven for 2 hours.

The actual piezoelectric filament production took place in a laboratory scale melt extruder. Detailed information on piezoelectric filament production from thermoplastic polymers can be found elsewhere [15-19]. In this study, high voltage applied to the filaments during polarisation was 15kV in the drawing area where the filaments were stretched 250% of their original length. The same parameters were also used to produce pristine PP filaments.

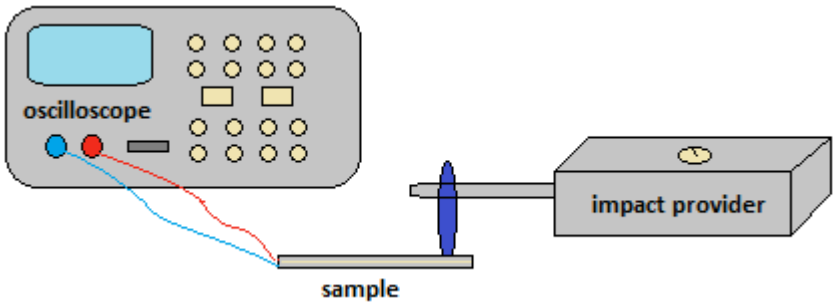

Figure 2. Schematically display of the experiment carried out to investigate the voltage outputs of the samples when subjected to the same impact created by a rotational mass.

Mechanical and thermal properties of the produced filaments were investigated via a tensile test equipment and a DSC, respectively. The obtained results for both pristine PP and PP/TM filaments

were comparatively studied. Voltage generation characteristic of the filaments were investigated by using a homebuilt equipment which provides a rotational impact onto the test sample as shown in Figure 2. The speed of the rotational impact provider unit could be controlled via the bottom on the top of it. For a comparative investigation, the speed of the rotational unit was fixed first and then the samples were located one by one. The voltage generated as a result of applied impact was recorded via an external storage device.

RESULTS and DISCUSSION

Pristine PP monofilaments and PP/TM monofilaments containing 1wt% of TM were produced to investigate the effect of draw ratio on tensile strength, crystallinity and voltage output of produced filaments. Obtained results from each test and experiment have been discussed in this section. Some mechanical properties of the filaments were tested via a tensile test equipment and the obtained result were given in Table 1.

Table 1. Some mechanical properties of produced monofilaments

	Units	**Pristine PP monofilament**	**PP/TM monofilament**
Elongation	%	150.04	105.28
Force	cN	246.12	270.01
Tenacity	cN/tex	14.55	15.63
Count	tex	16.91	17.28
Breaking time	sec	30.20	21.17

The count of the filaments were calculated by weighing the certain length of the filaments. Ten measurements were done for each type of filament and the average was taken as the count which was recorded as 16.91 tex for pristine PP and 17.28 tex for PP/TM filaments. Calculated counts were used as inputs for the tensile test equipment. Other values were directly taken from the tensile test equipment after ten measurements were conducted for each type of sample. As seen in the table, tenacity of PP/TM monofilaments were recorded as 15.63 cN/tex while pristine PP showed slightly lower tenacity, 14.55 cN/tex. However, general expectation is to see lower tensile properties of a filament when particles are added into polymer structure since they cause discontinuity.

Temperature dependent behaviours of the filaments were investigated under a DSC. The thermal test was carry out between -50°C and 200°C with 10°C increment per minute for each sample. Results such as melting temperature and melting enthalpy of the samples were obtained from the thermogram and the degree of crystallinity for each sample was calculated from the melting temperature (Tm), melting enthalpy (ΔHm) and degree of crystallinity (Xc) of the filaments. The results are given in Table 2. Tm and ΔHm were directly taken from DSC while Xc was calculated via the standard heat of crystallinity for 100% crystalline PP.

Table 2. Thermal characteristics of the filaments; melting temperature and melting enthalpy values were obtained from DSC, degree of crystallinity was calculated.

	Melting Temperature Tm (ºC)	**Melting Entalphy** ΔHm (J/g)	**Degree of Crystallinity** %
Pristine PP	163.6	77.39	37.02
PP/TM	163.2	85.24	40.78

As it can easily be detected from the Table 2 that an addition of TM particles has an influence on the degree of the crystallinity of the filaments due to the change in melting enthalpy. However, for further phase identification of the filaments an XRD analysis could be carried out since XRD provides the

information about the materials including but not limited to crystallinity, crystal structure of the material with interatomic distances and bond angles of the atoms, phase identity, phase purity etc.

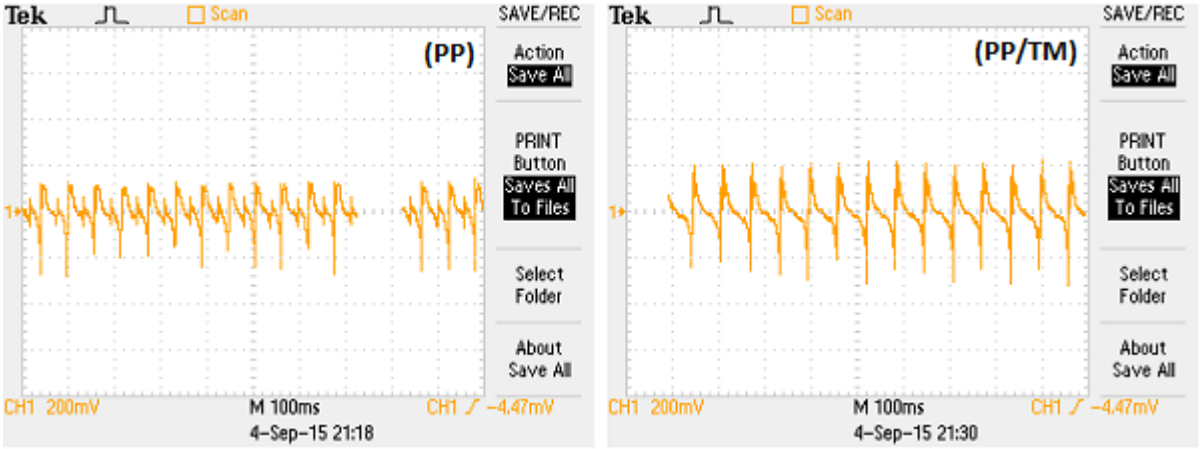

Figure 3. Voltage responses of produced samples under an applied rotational impact

A light impact created by a rotational mass was applied onto the prepared fiber composite samples for investigation of voltage response of the filament. Samples were immobilized from one end, where it was connected to the oscilloscope, and the other end was left free for oscillation. The data obtained from oscilloscope was recorded in an external data storage device. The voltage output results are given in Figure 3. Rotational impact test results showed that, addition of TM particles had an effect on voltage generation of the poled PP filaments. The comparison was done on the peak voltage output values of the samples. It was observed that the highest peak voltage generated by the sample containing PP filaments which was recorded as was 280mV while the highest peak voltage generated by the sample containing PP/TM filaments was recorded as 320mV.

CONCLUSIONS

In this study, PP and PP/TM monofilaments were produced via a laboratory scale melt extruder with a polarization unit placed in the draw zone. Production parameters were kept the same for both PP and PP/TM monofilament production. 250% stretching and 15kV high DC voltage were applied to the filaments at a temperature of about 80ºC. Tensile properties, crystallinity behavior and voltage response of the filaments were investigated. Comparative study on voltage outputs of the samples showed that samples produced from PP/TM monofilaments showed higher peak voltage generation than sample prepared from PP monofilaments. The peak voltage generation values were 280mV and 320mV for PP samples and PP/TM samples, respectively. It can be concluded that the voltage generation characteristics of PP piezoelectric materials can be contributed further with addition of appropriate additives. Since produced filaments showed acceptable mechanical properties, they can easily be used into textile structures for energy generating smart applications.

ACKNOWLEDGMENTS

The author acknowledges The British Council and TUBITAK for Newton-Katip Çelebi Grant, University of Bolton Staff for the permission to use their laboratories and Prof. Dr. Esra KARACA for providing TM particles. This study was supported by scientific activities participation program of Namık Kemal University.

REFERENCES

[1] Curie J, Curie P, Compt. Rend 1880, **91**, 383-386.

[2] Broadhurst M G, Davis G T, McKinney J E, Collins R E, J. Appl. Phys. 1978, **49**, 4992-4997.

[3] Zimmerman D, Northern Mariner 2002, **12**, 39-52.

[4] Nicolson A M, Trans. of the American Inst. of Elec. Engineers 1919, **38**, 1467-1493.

[5] Kawai H, Jpn. J. Appl. Phys. 1969, **8**, 975-976.

[6] Brain K R, Proc. Phys. Soc. 1923, **36**, 81-93.

[7] Fukada E, Ultrasonics 1968, **6**, 229-234.

[8] Slichter W P, J. Appl. Phys. 1958, **29**, 1438.

[9] Xu G, Clancy T C, Mattice W L, Macromolecules 2002, **35**, 3309.

[10] Marco T, Pasch H, Macromolecules, 2009, 42, 6063.

[11] Padden F J, Keith H D, J. Appl. Phys. 1959, **30**, 1479.

[12] Lovinger A J, Science 1983, **220**, 1115.

[13] Varga J, Polypropylene: Structure Blends and Composites 1995, Chapman&Hall, 56-115.

[14] Dickens B, Balizer E, DeReggi A S, Roth S C, J. Appl. Phys. 1992, **72**, 4258.

[15] Bayramol D V, Industria Textila 2017, **68**, 47-53.

[16] Bayramol D V, Sion N, Shah T, Qian L, Shi S, Smart Materials & Structures 2013, **22**, 075017.

[17] Siores E, Hadimani M L, Vatansever D, EP Patent: EP2617075 B1, 2014.

[18] Bayramol D V, Soin N, Hadimani R L, Shah T, Siores E, Journal of Nanoscience and Nanotechnology 2015, **15**, 7130-7135.

[19] Bayramol D V, Journal of Textiles and Engineer 2016, **23**, 166-171.

Corresponding author:

Derman VATANSEVER BAYRAMOL

Namık Kemal University, Corlu Faculty of Engineering, Department of Textile Engineering

E-mail: dvbayramol@nku.edu.tr

Presentation options to indicate

1. Indicate your preference for the presentation: ***Oral****.*

2. Indicate the preference for the ***conference topic****: Technical / Smart Textiles*

Paper submission

Papers will be submitted in word document format via email to bursa@kmo.org.tr after saving the paper under name of the corresponding author

The deadline for the abstract submissions is ***25 February 2017*** *and for the full text submissions is* ***15 April 2017****.*

Lif Destekli İletken PUR Kompozit Malzemelerin Tasarımı ve Üretimi

Design and Production of Fiber-Reinforced Conductive PUR Composite Materials

Devrim D. Soyaslan[1]

1Mehmet Akif Ersoy Üniversitesi, Müh-Mim.Fak., Polimer Müh., Burdur, Türkiye

E-mail adresi: dsoyaslan@mehmetakif.edu.tr

ÖZET

Çalışmanın amacı, iletken elyaf ve/veya iletken parçacıklar ile desteklenmiş elektromanyetik koruma etkinliği yüksek malzemeler tasarlamak ve geliştirmektir.

Bu amaç doğrultusunda, poliüretan (PUR) matrisli kompozit paneller tasarlanmış ve üretilmiştir. Bu çalışmada üretilen kompozit malzemelerde takviye elemanı olarak, karbon elyafı ve/veya nanokarbon metal tozları kullanılmıştır. Üretilen kompozit panellerin elektromanyetik koruma etkinlikleri belirlenmiş olup, bunun yanı sıra SEM görüntüleri alınmış ve birim ağırlıkları ile kalınlıkları da saptanmıştır. Elektromanyetik koruma etkinliği testleri, Elektromanyetik Koruma Etkinliği Ölçüm Kutusu (Clean room, Faraday Kafesi, Test Kutusu) kullanılarak 'levha-plaka ölçüm tekniği' ve modifiye edilmiş 'MIL-STD-285 test metodu' na göre 27 MHz-6 GHz frekans aralığında gerçekleştirilmiştir.

Çalışma sonucunda, kalınlıkları 3-9 mm ve yoğunlukları 0,61-1,6 g/cm 2 arasında değişen kompozit paneller elde edilmiştir. Yapılan testler neticesinde, her kompozitin farklı frekanslarda etkin oldukları belirlenmiştir. Her malzemenin farklı frekanslarda etkin olması, malzemelerin sahip oldukları özellikler neticesinde farklı davranışlar sergilediklerini ortaya koymuştur. 27 MHz-6 GHz frekans aralığında yapılan elektromanyetik ekranlama testlerde; kompozitlerden, 22 dB ile 83 dB arasında değişen koruma değerleri elde edilmiştir. Bu yapıların inşaattan, tıp, havacılık ve uzay bilimlerine kadar pek çok alanda kullanım olanağına sahip olacağı düşünülmektedir.

Anahtar kelimeler: Elektromanyetik kalkanlama, elyaf, polimer, kompozit, carbon

ABSTRACT

The aim of the work is to design and develop high-quality materials with electromagnetic shielding effect supported by conductive fibers and / or conductive particles.

For this purpose, polyurethane matrix composite panels have been designed and produced. Carbon fiber and / or nanocarbon metal powders were used as reinforcements in the composite materials produced in this study. The electromagnetic shielding activities of the composite panels produced were determined, as well as SEM images were taken and their unit weights and thicknesses were determined. Electromagnetic protection effectiveness tests were carried out in the frequency range of 27 MHz-6 GHz according to the 'plate-plate measurement technique' and the modified 'MIL-STD-285 test method' using the Electromagnetic Conservation Activity Measurement Box (Clean room, Faraday Cage, Test Box).

As a result of the study, composite panels having thicknesses of 3-9 mm and densities of 0.61-1.6 g / cm 2 were obtained. As a result of the tests made, it was determined that each composite is effective at different frequencies. The fact that each material is active at different frequencies reveals that the materials exhibit different behaviors due to the properties they possess. Electromagnetic shielding tests conducted on the frequency range 27 MHz to 6 GHz; Composites, protection values ranging from 22 dB to 83 dB were obtained. These constructions are thought to have many uses for the field, ranging from architecture to medicine, aviation and space sciences.

Key words: Electromagnetic shielding, fiber, polymer, composite, carbon

GİRİŞ

Çok büyük bir hızla gelişen teknoloji bazı olumsuzlukları da beraberinde getirmektedir. Günlük hayatımızda karşılaştığımız radyasyon kaynakları arasında; radyo, televizyon, telefon telsiz, radar ve uydu istasyonları vericileri, aktarıcıları, tesisleri, antenleri, baz istasyonları, terminalleri, link istasyonları, anten çiftlikleri ile yüksek ve orta gerilim hatları, trafo istasyonları, çeşitli cihaz ve ekipmanlar, evlerde kullanılan cihazlar, tıbbi tanı ve tedavide kullanılan cihazlar yer almaktadır [1]. Bunlardan en önemlisi giderek yaygınlaşan cep telefonu kullanımına bağlı olarak özellikle kentlerde sayıları giderek artan baz istasyonlarının insan sağlığı üzerindeki olumsuz etkileridir. [2-5]. Bu cihazların oluşturdukları elektromanyetik alanlara maruz kalan insanlarda zaman içinde pek çok hastalığın ortaya çıktığı, hatta kanser gibi ölümcül hastalıkların arttığı, yapılan pek çok araştırmada ortaya konmuştur. Bugün artık tüm dünyada elektromanyetik kirliliğin sağlık üzerindeki etkilerinin azaltılması amacı ile gerekli yasal düzenlemeler yapılmaya başlanmıştır [6-8].

Elektromanyetik dalgaların bütün bu etkileri göz önüne alındığında, elektromanyetik enerjilere karşı koruma oluşturabilecek uygun materyallere ihtiyaç duyulduğu ve bu materyallerin geliştirilmesinin büyük bir önem arz ettiği görülmektedir [9]. Böylece, günümüz inşaat sektörü için sadece yapı malzemesi özelliği taşımayıp, aynı zamanda elektromanyetik koruma etkinliğine de sahip materyallerin geliştirilmesi büyük öneme sahiptir [10].

Tekstil ürünlerinin elektromanyetik kalkanlama amacı ile kullanımı hem uluslararası hem de ulusal akademik ve sanayi çevrelerinde giderek artan bir ilgi ile karşılanan bir konudur. Bu ürünler yalnızca tekstil camiasında değil aynı zamanda pek çok endüstriyel alana hitap eden malzeme bilimi alanında da ilgi gören malzemeler olarak görülmeye başlanmıştır. Elektromanyetik kalkanlama özelliğine sahip tekstil yüzeyleri ile ilgili uluslararası düzeyde pek çok araştırma projesi yapılmakta ve ürün geliştirilmektedir. Tekstil ürünlerinin, insanoğlunun elektromanyetik dalgaların etkilerinden korunmasında son derece basit ve ucuz çözümler sunabileceği bilinmektedir [11,12].

Son birkaç yılda; elektrik ve elektronik alanında yapılan çalışmalarda, tekstil yapıları ve tekstil yapılarıyla desteklenmiş kompozit yapılar oldukça geniş yer tutmaktadır. Tekstil yapılarının, diğer yapılara oranla daha hafif, daha esnek ve mekanik dayanımlarının daha iyi olması; bu yapıların ve kompozitlerinin uzay ve havacılık endüstrisi, endüstriyel kullanımlar, spor malzemeleri, elektrik ve elektronik uygulamaları, inşaat alanı vs gibi pek çok alanda yaygın olarak kullanılmasını sağlamaktadır [11-13].

Materyallerin elektromanyetik koruma etkinliklerinin değerlendirilmesi amacıyla kullanılan çok sayıda standart ve metot mevcuttur. Bunlar test edilmek istenen materyale, materyalin boyutlarına, kullanım yerine göre ve frekans aralığına göre değişebilmektedir. Test ölçüm sistemleri temel olarak iki temel prensip üzerine dayanmaktadır. Bu metodlar ‘iletim kaybı yöntemi’ (transmission methot) ve ‘çift anten yöntemi’ (twin antenna method) dir. ‘İletim kaybı yöntemi’ düz plaka formundaki materyallerin koruma performansı değerlendirileceğinde kullanılırken, çift anten yöntemi hem düz formdaki materyallerin koruma performanslarının değerlendirilmesinde hem de bu materyalden yapılmış bir kafesin (enclosure) koruma performansının değerlendirilmesinde kullanılmaktadır. Bu metod ve standartlardan bazıları; ASTM D 4989 Coaxial transmission line, ASTM ES-7 Dual Chamber Test Düzeneği, ASTM ES-7 Coaxial Transmission line, NBS Flanged Coaxial Cell Test Düzeneği ve Modifiye MIL-STD-285 Test Metodu’dur (Kinningham, B.A. ve Yenni, D.M.1988). Bunun yanında çeşitli araştırmacıların kendi tasarladıkları test düzenekleri de, materyallerin elektromanyetik koruma performanslarının değerlendirilmesi amacıyla kullanılmaktadır [14,15].

DENEYSEL KISIM

Materyal

Bu projede üretilmesi planlanan yalıtım malzemelerinde, matriks malzeme olarak poliüretan polimeri kullanılmış olup, takviye elemanı olarak ise karbon elyafı, ve/veya nanokarbon metal tozları kullanılmıştır. Çalışma kapsamında karbon elyaf/ poliüretan matriks, ,nanokarbon toz/ poliüretan matriks ve karbon elyaf/nanokarbon toz/ poliüretan matriks olmak üzere üç farklı numune (kompozit

plaka) elde edilmiştir. Numune boyutları yapılacak testler göz önünde bulundurularak, 35×25 cm şeklinde planlanmış ve üretilmiştir (Şekil 1).

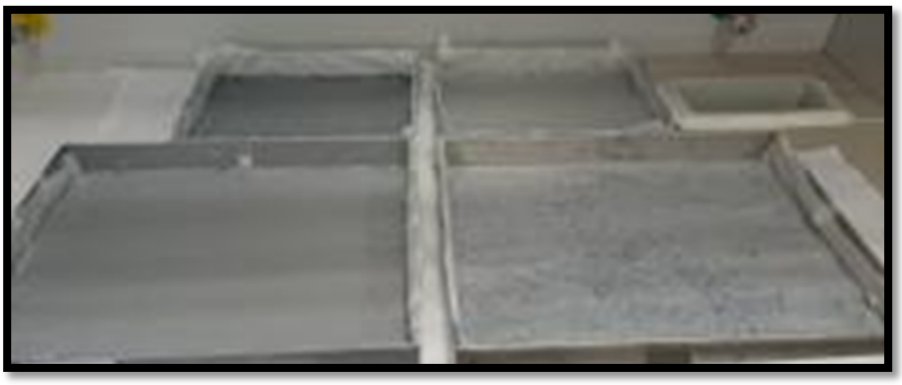

Şekil 1. Kompozit numuneler

Numune kalınlıkları, 0-25mmx0,01 hassasiyetli outside micrometer ile ölçülmüştür. Elde edilen numunelere ait özellikler Tab.1' de verilmiştir.

Tablo 1. Kompozit numunelere ait bilgileri içeren tablo

Numune No	Kalınlık (mm)	Yoğunluk (g/cm^2)	Karbon elyaf oranı (%)	Karbon toz oranı (%)
N1	4,68	0,655	-	-
N2	6,68	1,33	-	4
N3	8,4	0,755	0,5	-
N4	8,16	1,6	1	-
N5	4,15	1,14	0,5	0,5
N6	3,76	0,612	-	1

YÖNTEM

Kompozit Malzemelerin Üretimi

Viskozitesi yüksek sıvı haldeki matriks polimer içerisine elyaf takviyesi; elle yatırma yöntemi ile yapılmış ve karışım, laboratuvar tipi bir mikser yardımıyla sürekli karıştırılarak homojen hale getirilmiştir. Homojen hale gelen sıvı kompozit malzeme 35x25 cm boyutlarındaki metal kalıplara dökülerek katılaşmaya bırakılmış ve on dört günlük kürlenme sonucunda katı kompozit plakalar elde edilmiştir.

Elde edilen kompozit plakalara bazı fiziksel testler ile elektromanyetik kalkanlama testleri yapılmıştır.

Kompozit Malzemelerin Elektromanyetik Koruma Etkinliklerinin Tayini

Malzemelerin elektromanyetik koruma etkinliklerinin ölçümü, Elektromanyetik Koruma Etkinliği Ölçüm Kutusu (Clean room, Faraday Kafesi, Test Kutusu) kullanılarak 'levha-plaka ölçüm tekniği' ve

modifiye edilmiş ‘MIL-STD-285 test metodu’ na göre 30 MHz-6 GHz frekans aralığında gerçekleştirilmiştir (Şekil 2).

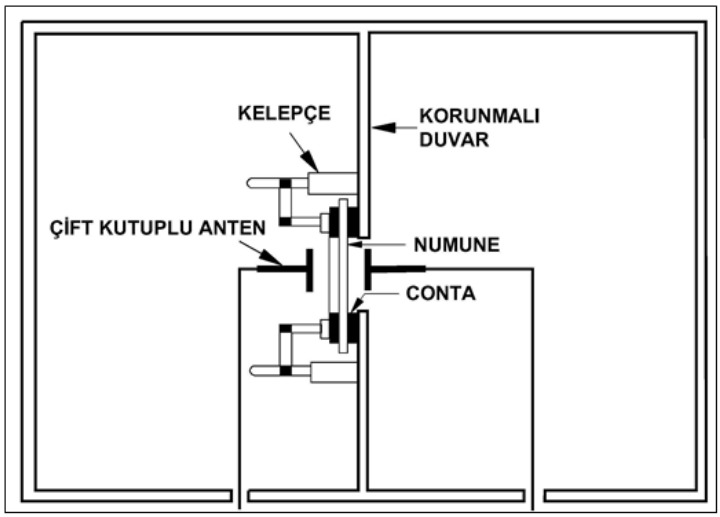

Şekil 2. Elektromanyetik Koruma Etkinliği Ölçüm Kutusu (Shielded room setup -modified MIL-STD-285 [16]

Modifiye MIL-STD-285 testi, plaka halindeki materyallerin SE ölçümlerinin yapılmasında kullanılan yöntemlerden biridir. Bu yöntemde, test edilecek numune, korumalı bir odanın duvarına açılmış bir deliğin üzerine yerleştirilir. Manyetik dalga yayan bir anten deliğin bir tarafına yerleştirilirken alıcı anten de deliğin diğer tarafına yerleştirilir. Ölçüm iki kademeli olarak yapılır. Önce deliğe numune yerleştirilmeden alıcı antene ulaşan değer (P_0) okunur, sonra araya numune yerleştirilerek alıcı antene ulaşan değer (P_1) okunur ve elektromanyetik koruma etkinliği değeri iletim kaybı tekniğine göre Denklem 1.1’e göre hesaplanır [17].

KE : Elektromanyetik koruma etkinliği,

P_0 : Numune yerleştirmeden alıcı antene ulaşan değer,

P_1 : Numune yerleştirilerek alıcı antene ulaşan değer olmak üzere,

$$KE = 10\log\left(\frac{P_0}{P_1}\right) \qquad (1.1)$$

BULGULAR VE TARTIŞMA

Fiziksel Bulgular

Tüm numunelerin yüzey görüntüleri incelendiğinde sadece karbon toz takviyeli kompozitlerin yüzeylerinin düzgün ve pürüzsüz, sadece elyaf katkılı ve elyaf/ toz takviyeli kompozitlerin yüzeylerinin dalgalı ve pürüzlü oldukları gözlenmiştir.

Aşağıda Şekil 3 ‘de SEM’de çekilmiş karbon lif ve/veya karbon toz destekli kompozit numunelere ait yüzey görüntüleri görülmektedir. Şekil.3 incelendiğinde, N1 numunesi ile diğer karbon lif ve/veya karbon toz takviyeli kompozit numunelere ait SEM görüntülerinin farklı olduğu görülmektedir. N2

numunesine ait SEM görüntüsünde karbon partikülleri ve N3, N4, N5 numunelerine ait SEM görüntülerinde de karbon elyaflar görülmektedir.

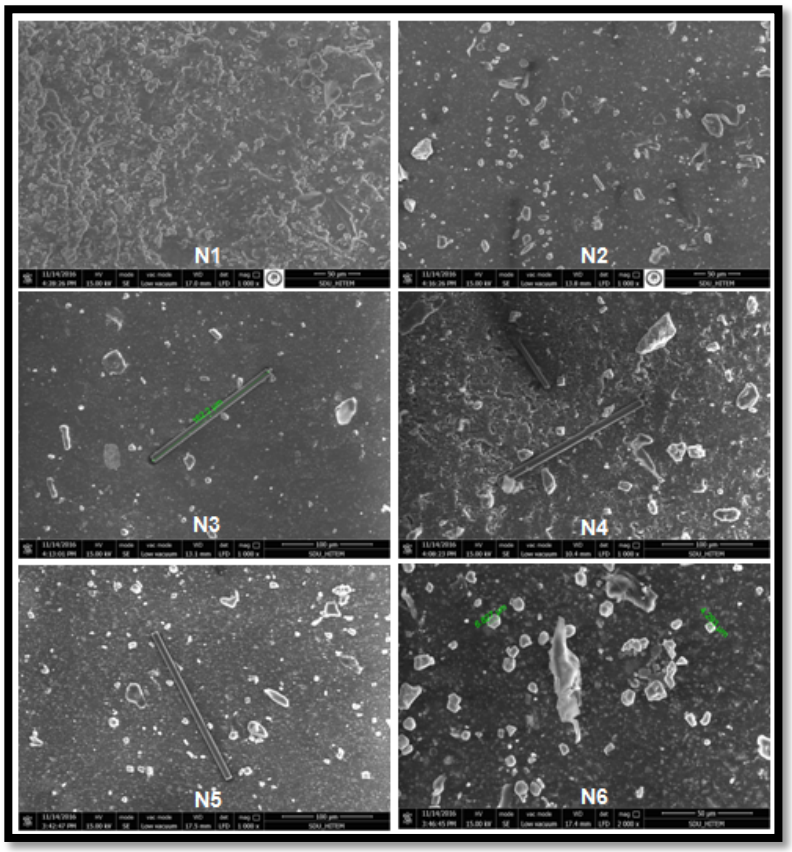

Şekil 3. Karbon lif ve/veya karbon toz destekli kompozit numunelere ait SEM görüntüleri

Kompozitlere Ait Elektromanyetik Koruma Etkinliği Performansı Bulguları

Aşağıda Tab. 2'de projede üretilmiş olan kompozitlere ait elektromanyetik koruma etkinliği performansı bulguları verilmiştir. Testler ilk olarak arada metal plaka varken kalibrasyon amaçlı yapılmış (tam dolu) sonra da arada numune yokken (boş) yapılmıştır. Daha sonra ise numuneler sırayla kutudaki boşluğa yerleştirilmişler ve test edilmişlerdir.

Tablo 2. Projede üretilmiş olan kompozitlere ait elektromanyetik koruma etkinliği performansı

Sıra No	Frekans(Mhz)	27	50	100	250	500	900	1000	1800	2400	2600	5000	6000
	Sinyal gücü (dBm)	2,5	3,3	3,5	3,3	3,8	3,1	3,4	2,9	2,1	0,8	-6	-8,6
	Numune Adı												
1	Numune 1	-37	-42,5	-30,5	-21	-34	-62	-72	-24,5	-20,5	-31	-48,5	-43
2	Numune 2	-39	-47	-31,5	-21	-31,5	-73	-74	-25,5	-31,5	-31,5	-51,5	-48
3	Numune 3	-37,5	-43	-32,5	-21,5	-42,5	-81	-83	-37	-55,5	-46,5	-73	-69
4	Numune 4	-37	-42,5	-32	-21,5	-41,5	-80	-83	-44,5	-63	-46,5	-90	-60
5	Numune 5	-37,5	-43,5	-31,5	-21,5	-44	-83	-85	-48	-44	-43,5	-75	-60,5
6	Numune 6	-37,5	-42,5	-31,5	-21	-32,5	-62	-72	-24	-26	-31,5	-54	-54
7	BOŞ	-36,5	-42,5	-32,5	-21	-35,09	-63,77	-72,32	-19,5	-20	31,68	-47,55	-50,64
8	Tam Dolu	-38,73	-42,5	-32,5	-21	-44,5	-86,14	-90	-61	-46	-55,5	-93	-84,36
	Frekans(Mhz)	27	50	100	250	500	900	1000	1800	2400	2600	5000	6000

değerleri

SONUÇLAR

Kompozit numunelerin yüzeyleri morfolojik olarak incelendiğinde, karbon lif destekli numunelerin yüzeyinde dalgalanmalar olduğu buna karşın nanokarbon toz destekli numunelerin yüzeyinin son derece düzgün ve pürüzsüz olduğu görülmüştür. Karbon lif takviyeli numunelerde, üretim esnasında matriks içerisinde homojen bir lif dağılımının sağlanması oldukça güç olmuş ancak nanokarbon toz takviyeli numunelerde son derece homejen dağılımlı bir kompozit malzeme elde edilmesi sağlanmıştır. Aynı miktardaki matriks yapısına, ağırlık olarak aynı miktarda ayrı ayrı karbon lif ve karbon toz eklenmiş numuneler karşılaştırıldığında karbon lif destekli numunelerde karbon liflerinin matriks yapısında bulunan sıvının bir kısmını absorbe ederek homojen dağılımı engellediği gözlenmiştir. Karbon toz ise matriks yapısındaki sıvıyı absorbe etmeden homojen bir şekilde dağılabilmiştir. Dolayısı ile, belirli bir miktardaki matriks sıvıya ağırlık anlamında daha fazla karbon toz ilave edilebilirken, aynı miktardaki matriks sıvıya daha az karbon lif ilave edilebilmiştir.

Kompozitlerin elektromanyetik koruma etkinliği değerlerine bakıldığında, her kompozitin farklı frekanslarda etkin oldukları belirlenmiştir. 27 MHz'de 39 dB ve 50 MHz de 47 dB lik koruma değeri ile N2 kompoziti en etkin malzeme olarak belirlenmiştir. 100 MHz 'de N3 numunesi 33 dB ile en etkin numune iken 250 MHz 'de N3, N4 ve N5 numuneleri 22 dB ile en etkin numuneler olmuştur. N5 kompoziti, 500 MHz, 900 MHz, 1000 MHz ve 1800 MHz frekanslarında en iyi korumayı sağlayan kompozit olmuştur. N4 kompoziti; 2400 MHz de 63 dB'lik, 2600 MHz'de 47 dB'lik ve 5000 MHz'de 90'lık koruma ile en iyi elektromenyetik koruma sağlayan malzeme olmuştur. N3 kompoziti ise 6000 MHz'de 69 dB'lik koruma ile en iyi koruma sağlayan malzeme olarak belirlenmiştir. Elde edilen tüm elektromanyetik koruma etkinliği test sonuçları değerlendirildiğinde; her malzemenin farklı frekanslarda etkin olduğu belirlenmiş ve bu durumun da, malzemelerin sahip oldukları kendilerine has özelliklerden dolayı meydana geldiği saptanmıştır.

Sonuç olarak, projede üretilen kompozit malzemeler fiziksel özellikleri ve elektromanyetik kalkanlama verimliliği açısından önemli değerlere sahip malzemeler olarak değerlendirilmişlerdir. Sonraki çalışmalarda bu malzemelerin ısı ve ses yalıtım özellikleri değerlendirilecek ve daha ileri malzemeler tasarlanacaktır.

KATKILAR

Bu çalışma MEHMET AKİF ERSOY Üniversitesi Bilimsel Araştırma Projeleri Komisyonu tarafından desteklenmiştir (Proje No: 194-NAP-13).

KAYNAKLAR

[1] Palamutçu S., Dağ N., Fonksiyonel Tekstiller I : Elektromanyetik Kalkanlama Amaçlı Tekstil Yüzeyleri, *Tekstil Teknolojileri Elektronik Dergisi* 2009, **3, 1,** 87-101.

[2] Kheifets, L, Monroe, J, Vergara, X., et al. Occupational electromagnetic fields and leukemia and brain cancer: An update two meta-analyses, *Journal Occup. Environ Med*., 2008, **50,** 677-88.

[3] Khurana V, Teo C, Kundi M, Hardell L, Carlberg M., Cell phones and brain tumors: A review including the long-term epidemiologic data, *Surg Neurol.,* **2009, 2**, (3), 205-14.

[4] Elvers, H., Jandrig B., Grummich, K., Tannert, C., Mobile phones and health: Media coverage study of German newspapers on possible adverse health effects of mobile phone use, *Health, Risk & Society*, 2009, **v 11, No 2**, 165-179.

[5] Ivancsits S, Diem E, Jahn O, Rüdiger H, Intermittent extremely low frequency electromagnetic fields cause DNA damage in a dose dependent way. *Int Arch Occup Env Health* 2003, **76**:431-436.

[6] Habash Rwy., Electromagnetic- the Uncertain Health Risk. *Potentials* 2003**, 22 (1)**, 23-26.

[7] Kasevich R.S., Cellphones, Radars, and Health, *Spectrum IEEE* 2002, **39 (8)**, 15-16.

[8]Williams T., The Health Effects of Electromagnetic Radiation, Electromagnetic Compatibility in Heavy Power Installations*, IEE Colloquium*: 1999, **23:5**/1-5/6.

[9] Tamburrano A., Sarto M.S., Electromagnetic Characterization of Innovative Shielding Materials ın the Frequency Range up to 8 Gigahertz*, IEEE Int.Symp.EMC***,** 2000**, 2,** 551-556.

[10] Hongtao, G., Shunhua, Liu, Yuping D., Ji C., Cement based electromagnetic shielding and absorbing building materials, *Cement & Concrete Composite* 2006, **28**, 468-474.

[11] Roh, S. W., Quan, Z. X., Nam, Y. D., Chang, H. W., Kim, K. H., Kim, M. K,, et al., Pedobacter agri sp. nov., from soil, *Int J Syst Evol Microbiol,* 2008, **58 (Pt 7),** 1640–3.

[12] Aniolczyk H, Koprowska J, Mamrot P, Lichawska J., Application of electrically conductive textiles as electromagnetic shields in physiotherapy, *Fibres& Textiles in Eastern Europe* 2004, **12**: 47–50.

[13] Araujo, G. G. L. de ; Moreira, J. N. ; Ferreira, M. de A. ; Turco, S. H. N. ; Socorro, E. P. do, Voluntary intake and performance of lambs fed with different manicoba hay dietary levels. *Rev. Ciencia Agron.* 2004, **35 (1)**: 123-130.

[14] Hock, O.T., Houw, F.C., Automated Shielding Effectiveness Test System For Shielded Enclosures, IEEE Symposium 2006, Pp: 682-685.

[15] Ogunsola, A., A Test Programme for the Shielding Effectiveness Evaluation of conductive Plastic Enclosures, IEEE Symposium 2000, Pp: 851-854.

[16] Kinningham, B.A., Yenni, D.M., Test Methods For Electromagnetic Shielding Materials, *IEEE Symposium, Session 4B* 1988, Pp: 223-230.

[17] Soyaslan, D. D., Elektromanyetik koruma etkinliğine Sahip Atkılı örme Kumaş ve Kompozitlerinin Geliştirilmesi, T:C. Süleyman Demirel Üniversitesi, *Fen Bilimleri Enstitüsü,* Isparta, 2009.

Sorumlu yazar:

Devrim Demiray SOYASLAN

Mehmet Akif Ersoy Üniversitesi, Mühendislik Mimarlık Fakültesi, Polimer Mühendisliği Bölümü

E-mail: dsoyaslan@mehmetakif.edu.tr

Sunumla ilgili belirtilmesi gerekenler

1. Sunumun niteliği sözlü sunumdur (Türkçe).

2. Konferans konuları içerisinde Teknik/Akıllı tekstiller konu başlığı altında değerlendirilebilir.

Shape Memory Performances of Fabrics Produced from Shape Memory Polyurethane Fibers Spun Under Different Conditions

S Aslan[1] and S Kaplan[1]

[1]Süleyman Demirel University, Engineering Faculty, Textile Engineering Department, Isparta, Turkey.

E-mail: selcukaslan0444@gmail.com

ABSTRACT

This study was focused on investigating shape memory performance of fabrics knitted from shape memory filaments and their potential for development of smart textiles. Six types of shape memory polyurethane (SMPU) fibers which were spun by wet spinning process using different spinning conditions with the existence of polyester gimped yarn. Shape memory performances of fabrics knitted from these filaments were determined by bagging test measuring shape fixity and shape recovery ratios. Bagging test results showed that, all shape memory fabrics produced under different spinning conditions could keep 37-58% of their bagged shapes after elastic recovery and 40-42% of the fixed deformation was recovered. As a result it is thought that, produced fabrics have sufficient shape memory performances sufficient for smart textile applications.

Key Words: shape memory polyurethane, wet spinning, knitted fabric, bagging test, shape memory behavior.

INTRODUCTION

Shape memory polymers (SMPs) can rapidly change their shape from a temporary deformed shape to permanent (or original) shape under appropriate stimuli such as temperature, light, electric field, magnetic field, pH, specific ion or enzyme [1]. In comparison to other shape memory materials, SMPs have been taking more attention for different end uses because of their properties such as high shape fixity and recovery, easy forming, adjustable transition temperature and good processability. SMPs are used in breathable textiles, medical textiles, protective garments etc. as fiber, film, coating and fabric forms [2,3]. SMP coated or laminated materials can increase the thermophysiological comfort of surgical protective clothing, bedding and incontinence products due to their temperature sensitive moisture management properties [2].

Shape memory polyurethanes (SMPU) are the most notable kind of SMPs and they have the advantage of broad switch temperature (glass transition or melting transition) by changing soft segment and hard segment type and contents [3,4]. Consequently, SMPU is the most widely used polymer among SMPs in textile applications [2]. SMPUs are phase separated due to the thermodynamic incompability between hard and soft segments and their morphology depends on the chemical composition and chain length of the soft segment. Thus, they exhibit remarkable shape memory effect. Many research groups have conducted studies about textile applications on shape memory polymers, mostly shape memory polyurethanes, with different forms such as fiber, yarn and film [5,6,7,8].

EXPERIMENTAL

Production of Shape Memory Fabrics

Shape memory fabrics were knitted with filaments which were spun from shape memory polyurethane (SMPU) by wet spinning process with different production conditions. SMPU polymer solutions were prepared with two different concentrations (20 % and 25 %) and coagulation bathes were prepared with three different concentrations (0 %, 1 % and 3 %) of DMF. Details of the filament spinning process can be found in a previous study [9]. Fabrics were produced by Lonati L462 circular knitting machine from spun SMPU filaments plied with gimped polyester yarn (90/10% SMPU/PES) and the mixture ratio in the fabric was about 90/10%. Yarn properties which were used in fabric production are summarized in Table 1.

Table 1. Production details of SMPU fabrics

Fabric code	Filament code (SMPU+elastane)	Coagulation bath concentration (%)	Polymer concentration in solution (%)	Yarn count (dtex)
SMF200	SMPU200	0	20	167
SMF201	SMPU201	1	20	111
SMF203	SMPU203	3	20	250
SMF250	SMPU250	0	25	84
SMF251	SMPU251	1	25	83
SMF253	SMPU253	3	25	139

A microscope image of a knitted shape memory fabric is shown in Figure 1.

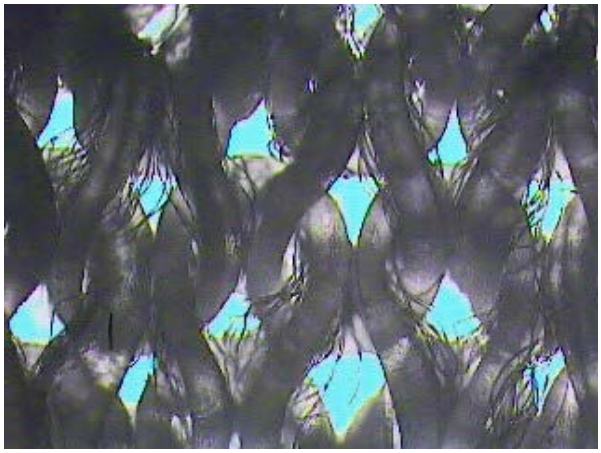

Figure 1. Microscope image of shape memory fabric

Shape Memory Performance of Fabrics

The shape memory behavior of knitted fabrics were investigated by a bagging test procedure applying multidirectional deformations on fabric. Bagging is a spherically-shaped and three-dimensional deformation of cloth or garments which involves complex deformations including tension, shearing, bending, and compression of a cloth along different directions [6]. Bagging performance of the fabrics were determined by deforming the fabric to a certain height and investigating its change under and above

the glass transition temperature (T_g) of the SMPU. The bagging test was carried out in a temperature controlled environment with a Lloyd LR5K tensile tester.

The details of bagging and shape recovery processes are shown in Figure 2. A sample of shape memory fabric with a diameter of 80 mm was used for the test. Steps of the bagging test procedure of shape memory fabrics are as follows:

1. The shape memory fabric was placed on a circular plate having diameter of 5 cm.
2. The environmental temperature was raised to 40°C and the steel ball was moved at a speed of 150 mm/min in order to form a bag shape of 5 cm high on fabric.
3. Fabric and ball temperatures were cooled down to environmental temperature (20±2 °C) and the fabric was hold under the applied tension for 3 minutes in order to fix temporary bag shape.
4. The ball was removed over the fabrics which was fixed to temporary bag shape and it was hold for 2 minutes for observing the elastic recovery. Then, first measurement was made to calculate shape fixity ratio of the fabric.
5. In the last stage, the environmental temperature was raised again to 40 °C and a total of three bag heights were recorded with one minute intervals to determine shape recovery ratio of the fabrics.

Figure 2. Bagging test steps of shape memory fabrics

Shape fixity (R_f) and shape recovery (R_r) ratios (%) of the fabrics were calculated to evaluate the performance of the bagging deformations according to Equations 1 and 2. Maximum bagging (ε_{max}) and residual bagging (ε_u, $\varepsilon_p(T)$) are the principle components in the equations as shown below:

$$R_f = \frac{\varepsilon_u}{\varepsilon_{max}} \times 100 \quad (1)$$

$$R_r = \frac{\varepsilon_{max} - \varepsilon_{p(T0)}}{\varepsilon_{max}} \times 100 \quad (2)$$

where R_f – bagging fix ratio; R_r – bagging recovery ratio; ε_{max} – maximum bag height; ε_u – residual bagging after unloading; ε_p (T_0) – residual bagging after test procedure under T_0 temperature ($T_0 < T_g$).

RESULTS and DISCUSSION

Shape memory performances of bagging test results of the fabrics produced from filaments spun using different polymer and coagulation bath concentrations are given in Figure 3. As can be seen in Figure 3 the bag height rapidly decreases after elastic recovery. The residual bag heights of shape memory fabrics, which were measured after elastic recovery were between 18-28 mm, resulting fixity ratios around 37-58%. When environmental temperature was increased for shape recovery, bag heights were measured between 7.5-11.25 mm after 3 minutes. These values correspond average shape recovery ratios of 40-42% for different fabrics having different spinning conditions. According to the calculated ratios, it can be said that the shape memory performance of fabrics are sufficient but slightly lower than the values in the literature [6]. This result may be attributed to the plied PES gimped yarn constituting 10% of the used yarn. The shape recovery performance may be affected as the SMPU filament should carry the PES gimped yarn during recovery process. Moreover, possible fiber breaks and friction/entanglement between the fibers, may have caused the mentioned result.

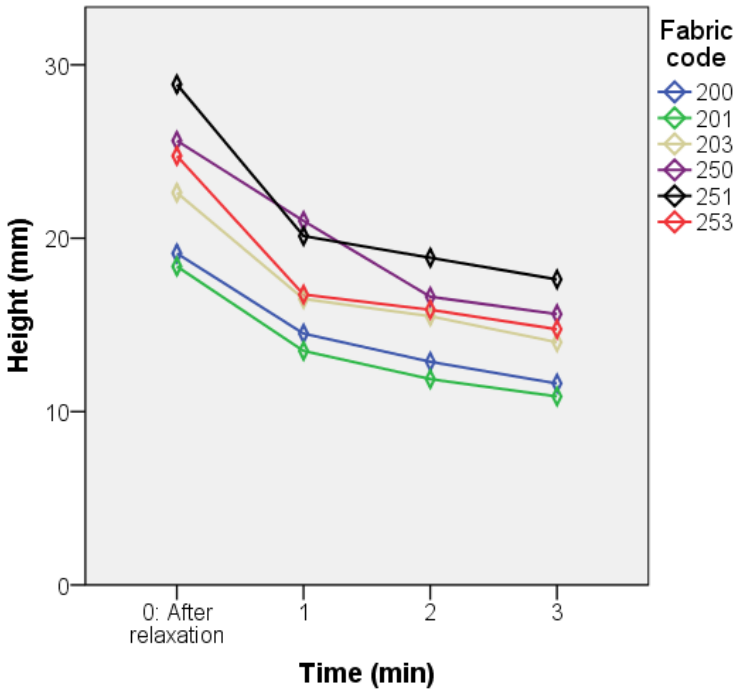

Figure 3. Bagging recovery performance of shape memory fabrics

The time dependent change in the shape of the deformed shape memory fabric as a result of temperature application is shown in Figure 4.

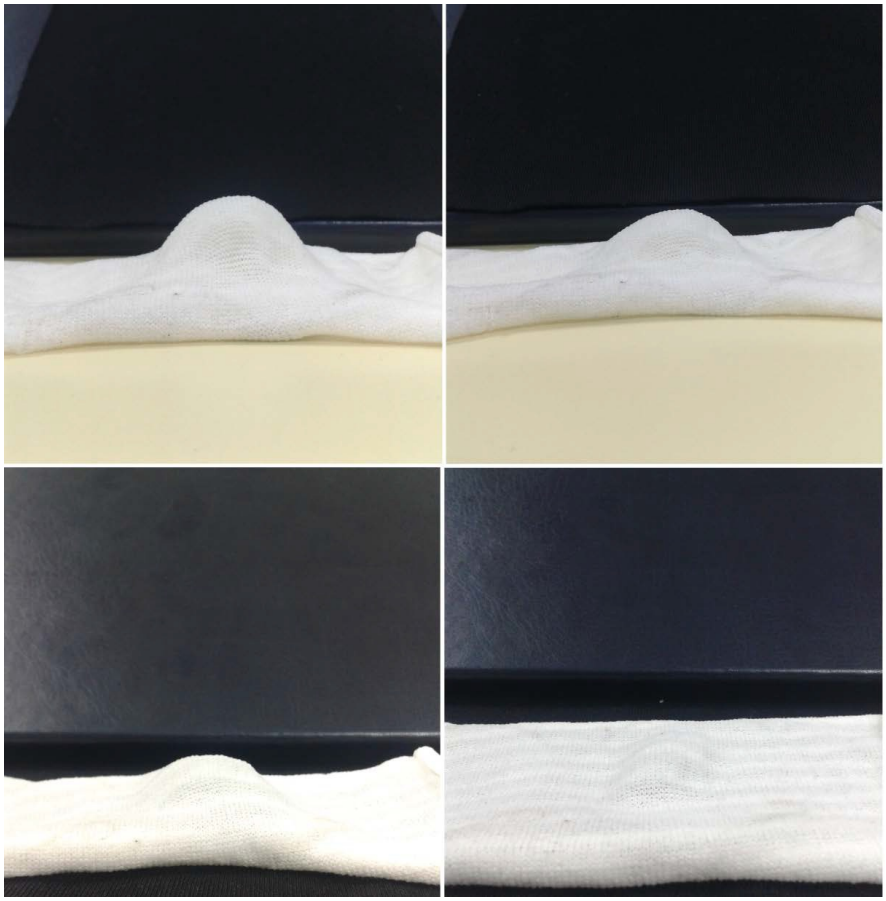

Figure 4. Shape changes of shape memory fabric during bagging test procedure

According to the statistical analyses results of bag height fixed on the fabric after elastic recovery, statistically significant differences were found between different shape memory fabrics ($p<0.05$). Accordingly, it was found that SMF251 fabric produced with filament which was spun with 25% polymer concentration and 1% coagulation bath concentration had the highest shape fixity ratio of 58%. This means that, it could keep the deformed bag height of 50 mm at the highest rate. SMF200 and SMF201 fabrics produced from filaments spun with 20% polymer concentration, 0% and 1% concentration of coagulation bath respectively, had the lowest bag heights ranging between 38-37% (Figure 5). Generally, fabrics produced from filaments having high polymer concentration (25%) showed better shape fixity performances. It was determined that the coagulation bath concentrations used in spinning of shape memory fibers had no effect on the shape fixity performances of fabrics.

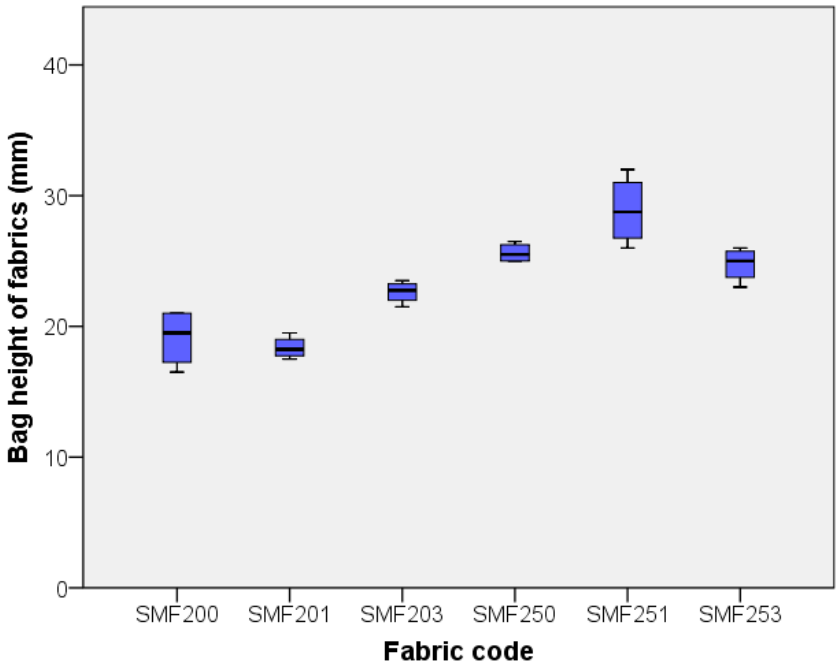

Figure 5. Box-plot diagram of bag height fixed on fabrics after elastic recovery

During the bagging test performed to determine shape memory performance of fabrics, when the press ball reached to maximum height (50 mm), the tension occurring on the fabrics was recorded and the tension of fabrics at a certain distance were evaluated. Figure 6 shows boxplot diagram of stress values (N) of fabrics under load. It was determined that SMF201 fabric has significantly lower stress value than other shape memory fabrics.

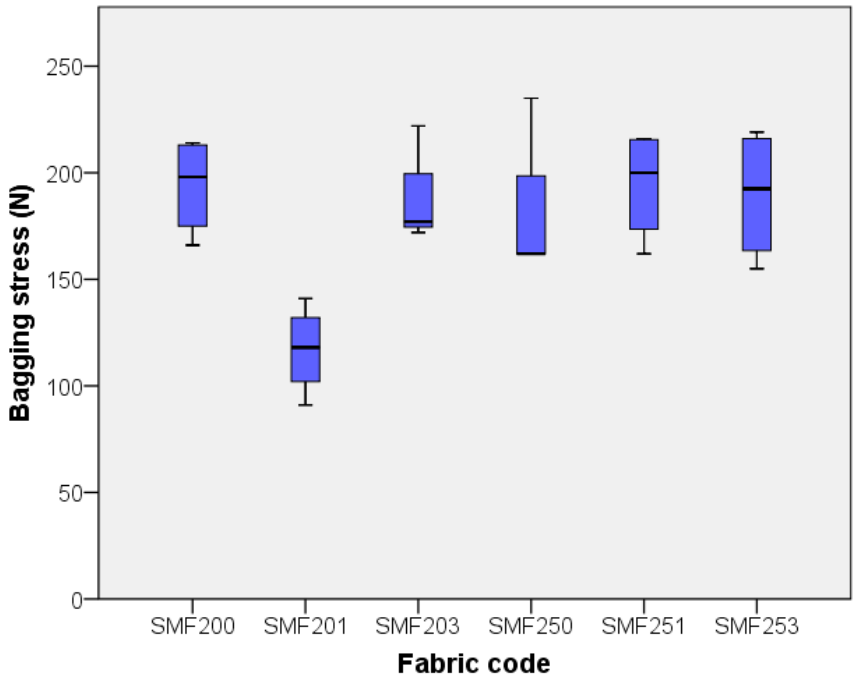

Figure 6. Boxplot diagram of the stress values of shape memory fabrics during bagging test

CONCLUSION

In this study, shape memory performances of fabrics which were produced with spun shape memory polyurethane fibers with the existence of polyester gimped yarn were evaluated by bagging test. According to test results, fabrics were showed remarkable shape memory performances. All fabrics were found to have shape fixity ratios ranging 40-42% and it was determined that SMF251 fabric produced from fiber, which was spun with 25% polymer concentration and 1% coagulation bath concentration had the highest shape fixity ratio of 58%. It was also observed that shape memory fabrics produced from fibers having high polymer concentration had higher shape fixity ratios ranging 50-58% than other fabrics. Moreover, solvent concentration in coagulation bath did not have a significant effect on the shape fixity ratios of fabrics. Summing up, it is believed that the fabrics produced in this study have sufficient shape memory performances and may be used in smart garments such as thermal protective clothing, sportswear, underwear, socks and gloves.

ACKNOWLEDGMENTS

This study was funded by a project of Suleyman Demirel University Scientific Research Projects Coordination Unit (4393-D2-15). We want to thank for their support.

REFERENCES

[1] Meng Q, Hu, J L, Composites: Part A 2009, **40**, 1661.
[2] Hu J L, Woodhead Publishing Limited 2007, 361p, Cambridge.
[3] Meng Q, Hu J L, Zhu, Y., Lu, J., Liu, B., Textile Research Journal 2009, **79**, 1522.
[4] Ahmad M, Xu B, Purnawali H, Fu Y, Huang W, Miraftab M, Luo J, Applied Sciences 2012, **2**, 535.
[5] Khan F, Koo J H, Monk D, Eisbrenner E, Polymer Testing 2008, **27**, 498.
[6] Liu Y, Lu J, Hu J L, Chung A, The Journal of The Textile Institute 2013, **104**, 1230.
[7] Meng Q, Hu J L, Polymers for Advanced Technologies 2008, **19**, 131.
[8] Matsumoto H, Ishigura T, Konosu Y, Minagawa M, Tanioka A, Richau K, Kratz K, Lendlein A, European Polymer Journal 2012, **48**, 1866.
[9] Aslan S, Kaplan S, Vlakna a Textil (Fibers and Textiles), 2017, **1**, 25.

Corresponding author:

Selçuk ASLAN

Süleyman Demirel University, Engineering Faculty, Textile Engineering Department, Isparta, Turkey

E-mail: selcukaslan0444@gmail.com

Presentation option: Oral presentation (Turkish)

Topic: Technical / Smart Textiles

Production and Analysis of Cellulose Nanowhisker Reinforced Thermo-water Responsive Polyurethane Nanocomposites

Nazife KORKMAZ MEMİŞ and Sibel KAPLAN

Süleyman Demirel University, Textile Engineering Department, Isparta, Turkey
nazifekorkmaz@sdu.edu.tr

ABSTRACT

In this study, shape memory-polyurethane was reinforced with cellulose nanowhiskers (CNWs) to create heterogeneous-twin-switch shape memory effect (thermal and water responsiveness simultaneously) and chemical/mechanical characterization of the produced polymeric nanocomposite films were conducted. Recently, there are attempts to modify SMPUs to have a switching temperature within the range of body temperature and create dual responsive structure that can be stimulated by different stimuli such as temperature and moisture. This study covers modification of SMPUs which has a transition temperature suitable for body applications by CNWs to possess water-sensitive shape memory effect besides its thermal stimulation by an easier process than synthesis of the polymer. Nanocomposite solutions with varying CNW concentrations (5, 10 and 20 wt%) were produced by solution blending and nanocomposite films were subsequently prepared by solution casting method. Fourier transform infrared (FT-IR) analysis was performed for characterization and effects of CNW on the mechanical and shape memory performances of films were investigated by tensile and thermo-aqueous programming test. According to FT-IR analysis results, peaks belonging to cellulose became visible in films with the increase of the CNW content. Strength and elongation at break increased until 10 wt% CNW concentration but a decrease was observed for 20 wt% concentration. Thermal-aqueous test results show that 20 wt% CNW including film had the maximum shape fixity value of 69.3% and minimum values of 48.5 % were calculated for neat SMPU. The maximum total shape recovery ratio of 91.45% was also obtained for 20 wt% CNW and 80.41% of this recovery belongs to water-induced shape memory effect. Summing up, besides maintaining thermal-induced shape recovery effect originally existing in their structure, it was observed that produced nanocomposites simultaneously possessed water-induced shape memory effect due to the percolation network of the cellulose whiskers whose hydrogen bonding can be regulated by water reversibly.

Key words: Shape memory polyurethane, cellulose nanowhiskers, nanocomposite, thermal sensitive, water/moisture sensitive, shape memory effect.

INTRODUCTION

The academic and industrial interest in the development of stimulus-responsive materials which enable a variety of functions and applications is steadily increasing in recent days [1]. Among these materials, shape memory polymers (SMPs) are very important smart materials having the capability to return their original (permanent) shapes from a temporary shape under appropriate external stimulus such as temperature, light, electric field, magnetic field, pH or water/moisture [2-4]. Most studies of SMPs focus on thermal induced structures because of their wide possible applications in different fields [5]. Among the thermal induced SMPs, segmented shape-memory-polyurethanes (SMPUs) have gained much popularity with the knowledge database, their wide range of transition temperatures, ease in shape ability and accessibility on a laboratory as well as a commercially viable scale [6]. For this reason, in recent years there are attempts to modify SMPUs to have a switching temperature within the range of body temperature and create dual responsive structure that can be stimulated by different external stimulus. The glass transition (T_g) of the SMPU is the switch temperature to fix the shape of the film (below and above the thermal transition temperature). Above the T_g, SMPU recovers to the original shape under the entropic elasticity of the network. At this point, water-induced SMPs

exhibiting lower transition temperatures with water in the polymer matrix has attracted attention. In such SMPs, water molecules penetrate into the amorphous region of the polymer and enable shape recovery at a lower temperature with disrupting intermolecular hydrogen bonds, plasticizing, and reducing the glass transition (T_g) temperature [7, 8]. However, water-induced SMPs have some disadvantages such as low elastic modulus, stiffness and strength properties, long shape recovery time due to slow diffusion process and difficulty in removing water absorbed by the polymer. In recent years, the formation of nanocomposite materials by introducing nanoparticles as reinforcing filler and/or the switching element is very useful design approach to modify the characteristics of shape memory polymers and obtain the water-induced SMPs.

Cellulose, as the most abundant polysaccharide on Earth, has been widely studied in different nano-forms, named as nanocrystal, nanowhisker, or short nanofiber, mainly for the fabrication of water responsive hybrids in virtue of its stiffness, high strength, and large surface area [9]. CNWs have nearly perfect crystalline structures where the cellulose chains are arranged compactly with strong hydrogen bonding interactions. According to the findings in literature, the introduction of CNWs into a SMPU matrix would afford nanocomposites with the water-induced shape memory depending on the percolation network formed by CNWs whose hydrogen bonds which can be reversibly regulated by water molecules [11, 12]. The structure of the CNW-SMPU nanocomposites featuring heterogeneous-twin-switches was illustrated in Figure 1.

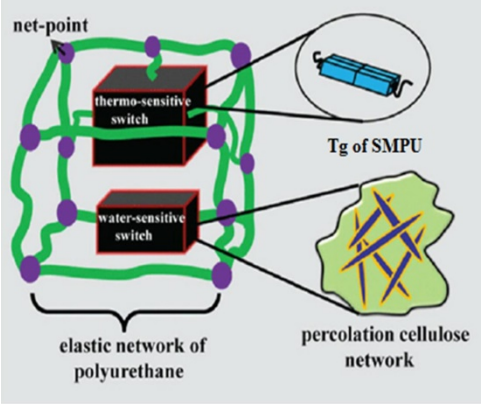

Figure 1. The structure of the CNW-SMPU nanocomposite films featuring heterogeneous-twin-switches.

Based on these mentioned advances and speculation about reinforcement of SMPU with CNWs, it was aimed to investigate modification SMPUs which has a transition temperature suitable for body applications by CNWs to create twin-switch smart materials to enhance its application areas in case of thermal comfort. In this way, a simpler method than synthesis of a dual function polymer was introduced. SMPU nanocomposite films including different amounts of CNW were produced to investigate their shape memory performances for both temperature and moisture. Besides FT-IR analyses, mechanical changes on the films with the incorporation of CNW were determined. Moreover, thermo-aqueous test cycle including a multi-stage procedure including shape memory tests under different thermal and moisture conditions (thermal environments below and above transition temperature (T_g) of SMPU, dry and aqueous environments).

EXPERIMENTAL

Materials

Pellet-type MM-3520 SMPU (SMP Technologies Inc. Japan) was used as matrix material to produce nanocomposite films. The particular SMPU is ester-based thermoplastic polyurethane SMP obtained from the Mitsubishi Heavy Industries (MHI), Japan which has a T_g of 35 °C according to producer

data. CNWs were supplied directly from the Nanolinter® in Turkey, having the following known average characteristics; a length of 223.90 nm and width of 35.72 nm (by TEM) and crystallinity 98.98% (by XRD). N, N-dimethylformamide (DMF) as solvent was purchased from Sigma-Aldrich. All chemicals are analytical grade and were used as received without further purification.

Fabrication of CNW-SMPU nanocomposite films

The CNW-SMPU nanocomposite films were produced by introducing CNWs as nanofiller into a SMPU matrix. For this aim first of all, SMPU was dissolved in DMF at a concentration of 5 wt% at 60 °C for 6 h. A 0.5 wt% dispersion of the CNWs in DMF was prepared by ultrasonic treatments using a sonifier (Sonopuls HD 2200, Bandelin Sonopuls Corp.) at 40% amplitude and 3-s on/off cycles for 1 h until dispersion became visually homogenous. A series of nanocomposite films with varying CNW concentrations, ranging from 0-20 wt% was produced by solution blending CNWs and the SMPU. The compositions of all nanocomposites prepared and studied were compiled in Table 1. The nanocomposite films were subsequently prepared by solution casting method by casting into glass petri dishes. In order to prevent thermocapilary instability on the film surface which causes surface roughness, the films then dried at 60 °C for 12 h. The final residual solvent was removed under vacuum at 80 °C for another 12 h (to ensure full removal of the DMF). Then the glass petri dishes were taken out from the vacuum oven and kept at room temperature for 2 h. The nominal thickness of the nanocomposite films were about 0.2 mm. The volume fraction (vol %) of CNW in the nanocomposites was calculated based on their weight fraction (wt.%) in the SMPU polymer, using a density of 1.5 g/cm^3 for the CNWs and a density of 1.25 g/cm^3 for SMPU.

Table 1. Composition of the nanocomposite film samples.

	Nanofiller content	
Samples	**wt (%)**	**v (%)**
SMPU	0	0
SMPU-CNW-5	5	4.17
SMPU-CNW-10	10	8.33
SMPU-CNW-20	20	16.67

Methods

FT-IR spectroscopy analysis

The Perkin Elmer Spectrum BX of Fourier Transform Infrared Spectrophotometer was used to investigate chemical compositions of the nanocomposite films. The spectroscopic analysis of the nanocomposite film samples were examined by KBr technique. The scanning range was between 4000 and 400 cm^{-1}during FT-IR analysis.

The tensile strength test

The effects of CNW on the mechanical performance of films were investigated by tensile test according to ASTM D-638 using the Lloyd LR5K Plus Electronic Tensile Testing Machine. The tensile test was conducted under standard atmospheric conditions (20 ºC and 65 RH %) with a rectangular strip of film samples with dimension of 40 x 10 x ~ 0.2 mm and crosshead speed of 10 mm/min. For each sample, an average of five tests was reported.

Shape memory properties investigation

The shape memory properties of CNW-SMPU nanocomposite films were conducted according to specially designed mechanical- thermo-aqueous programming tests. This test covers a multi-stage

procedure including shape memory tests under different thermal and moisture conditions (thermal environments below and above transition temperature (T_g) of SMPU, dry and aqueous environments). The mechanical-thermo-aqueous programming tests for multi-shape effects of the CNW-SMPU nanocomposites were performed manually by immersing a rectangular strip of film samples having dimension of 40 x 10 x ~ 0.2 mm into hot water (40 °C) while they were extended by 50% for 10 minutes. After giving the temporary shape (A), the film samples were cooled down to the room temperature and dried in vacuum for 24 hours for calculating their shape fixity ratios. In this stage both of the twin-switches were locked as the deformation was carried out in hot water. In the second stage, the composite film samples recovered to the second temporary shape (B) by heating up above 40 °C, T_g (switch temperature) of SMPU. At the end of the test, the composite film samples recovered from shape B to the original shape (C) by immersion into hot water (40 °C) which gave rise to the twin-switches unlocked together and allowed the full recovery [13].

According to these conditions, four different states were occurred due to the individual situation of twin switches. Each switch point in the nanocomposite structure could be turned 'on' or ''off'' according to thermal and water conditions. In dry-state, the percolation cellulose network which is formed between CNWs with strong hydrogen bonding via -OH groups of the cellulose was called in the state of 'switched on' and this effect is associated with the shape fixing. In wet-state, the hydrogen bonding between the CNWs was disrupted by the absorbed water molecules and called in the state of 'switched off' associating with the shape recovery. Like as the water responsive switch, below the T_g temperature soft segment of SMPU was called 'locked' and above T_g of SMPU was called ''opened''.

Beside these, the characteristics of the CNW-SMPU composites in tensile behaviors were described using a spring-twin switch model in literature (Figure 2). In this description, the spring showed the intrinsic elasticity of the SMPU and .switch 1 was thermal sensitivity, sourced from T_g of SMPU the switch 2 was water sensitivity sourced from the coupling-decoupling of hydrogen bonding of the percolation cellulose network (PCN).

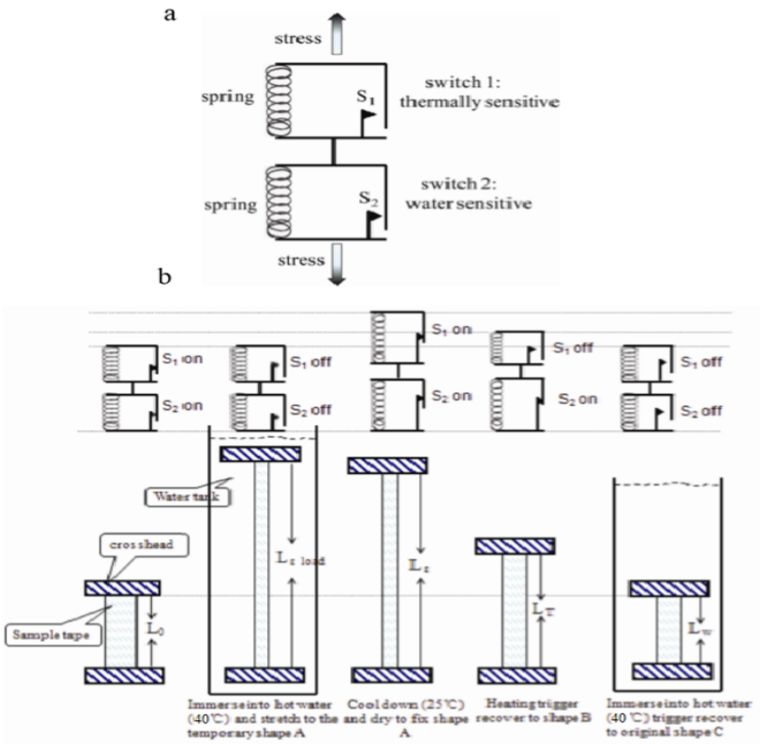

Figure 2. Spring-twin-switches model of the CNW-SMPU nanocomposite films (a), Extension, shape fixing and shape recovery of the nanocomposite films in a mechanical-thermo-aqueous programming tests (b).

The total shape fixity ratio (R_f) and shape recovery ratio (R_r) were calculated according to the below formulas.

$$R_f = \frac{L_\varepsilon - L_o}{L_{\varepsilon,load} - L_o} \quad (1)$$

$$R_r = \frac{L_{\varepsilon,load} - L_\omega}{L_{\varepsilon,load} - L_o} \quad (2)$$

In the formulas, $L_o, L_{\varepsilon,load}$, L_ε and L_ω represented for the original length, the extended length under stress, the fixed length of free stress and final length triggered by hot water respectively. Additionally, the total shape recovery in the program included two sequential parts of thermally-induced and moisture-induced recovery respectively. The percentage of the water-induced recovery against the total shape recovery was calculated with index p, which was defined as below;

$$p = \frac{L_T - L_\omega}{L_\varepsilon - L_\omega} \times 100(\%) \quad (3)$$

where L_T represented the length subjected to the thermally-induced recovery.In order to quantitatively evaluate the effect of CNWs on the shape recovery of the dry-state CNW-SMPU nanocomposites, R_f and R_r were calculated according to the below formulas;

$$R_f = \frac{L_\varepsilon - L_o}{L_{\varepsilon,load} - L_o} \quad (4)$$

$$R_r = \frac{L_{\varepsilon,load} - L_T}{L_{\varepsilon,load} - L_o} \quad (5)$$

RESULTS and DISSCUSIONS

FT-IR analysis (Figure 3) of the nanocomposite films with varying CNW concentrations show that the characteristic peaks of cellulose have become evident with an increase in the rate of cellulose incorporation. This increase in the peak intensity could be attributed to CNC content which was proved by the overlapping with the OH stretching vibration band. It has been observed that the peaks belonging to cellulose about 900 to 1200 cm^{-1} and 3200 to 3600 cm^{-1} became visible in films with the increase of CNW amount.